Received: 3 October 2023 | Revised: 5 November 2023 | Accepted: 6 November 2023

DOI: 10.1111/ppl.14100

ORIGINAL RESEARCH

Physiologia Plantarum

Etioplasts are more susceptible to salinity stress than chloroplasts and photosynthetically active etio-chloroplasts of wheat (*Triticum aestivum* L.)

Roumaissa Ounoki[1] | Adél Sóti[1] | Renáta Ünnep[2] | Gábor Sipka[3] | Éva Sárvári[4] | Győző Garab[3,5] | Katalin Solymosi[1]

[1]Department of Plant Anatomy, Institute of Biology, Faculty of Science, ELTE Eötvös Loránd University, Budapest, Hungary

[2]Neutron Spectroscopy Department, HUN-REN Centre for Energy Research, Budapest, Hungary

[3]Institute of Plant Biology, HUN-REN Biological Research Center, Szeged, Hungary

[4]Department of Plant Physiology and Molecular Plant Biology, Institute of Biology, Faculty of Science, ELTE Eötvös Loránd University, Budapest, Hungary

[5]Department of Physics, Faculty of Science, University of Ostrava, Ostrava, Czech Republic

Correspondence
Katalin Solymosi,
Email: katalin.solymosi@ttk.elte.hu

Funding information
Grantová Agentura České Republiky, Grant/Award Number: GA ČR 23-07744S; Nemzeti Kutatási Fejlesztési és Innovációs Hivatal, Grant/Award Numbers: FK124748, PD138540; Nemzeti Kutatási, Fejlesztési és Innovacios Alap, Grant/Award Number: New National Excellence Program ÚNKP-23-5-ELTE-12; Tempus Közalapítvány, Grant/Award Number: Stipendium Hungaricum Scholarship to R.O.

Edited by A. Krieger-Liszkay

Abstract

High soil salinity is a global problem in agriculture that directly affects seed germination and the development of the seedlings sown deep in the soil. To study how salinity affected plastid ultrastructure, leaf segments of 11-day-old light- and dark-grown (etiolated) wheat (*Triticum aestivum* L. cv. Mv Béres) seedlings were floated on Hoagland solution, 600 mM KCl:NaCl (1:1) salt or isosmotic polyethylene glycol solution for 4 h in the dark. Light-grown seedlings were also treated in the light. The same treatments were also performed on etio-chloroplasts of etiolated seedlings greened for different time periods. Salt stress induced slight to strong changes in the relative chlorophyll content, photosynthetic activity, and organization of thylakoid complexes. Measurements of malondialdehyde contents and high-temperature thermoluminescence indicated significantly increased oxidative stress and lipid peroxidation under salt treatment, except for light-grown leaves treated in the dark. In chloroplasts of leaf segments treated in the light, slight shrinkage of grana (determined by transmission electron microscopy and small-angle neutron scattering) was observed, while a swelling of the (pro)thylakoid lumen was observed in etioplasts. Salt-induced swelling disappeared after the onset of photosynthesis after 4 h of greening. Osmotic stress caused no significant alterations in plastid structure and only mild changes in their activities, indicating that the swelling of the (pro)thylakoid lumen and the physiological effects of salinity are rather associated with the ionic component of salt stress. Our data indicate that etioplasts of dark-germinated wheat seedlings are the most sensitive to salt stress, especially at the early stages of their greening.

1 | INTRODUCTION

Plastids, originating by endosymbiosis between an ancient heterotrophic eukaryotic host and an ancient photosynthetic cyanobacterium, are plant organelles responsible for photosynthesis. In the absence of light, the proplastids of angiosperm plants differentiate into a special plastid type, the so-called etioplasts. These plastids are characterized by the absence of chlorophyll (Chl) pigments and the presence of a peculiar cubic phase membrane system, the so-called prolamellar body (PLB) connected to flat prothylakoids (PTs) (Ryberg & Sundqvist, 1982). The major chlorophyllous pigment in etiolated plants is the Chl precursor protochlorophyllide (Pchlide). Pchlide is

the substrate of the NADPH:protochlorophyllide oxidoreductase (POR) responsible for the light-activated reduction of Pchlide into chlorophyllide (Chlide) (Solymosi & Schoefs, 2010), which is then esterified to produce Chl. In parallel, light induces the dispersal of the PLB and its relatively quick transformation into flat thylakoid membranes, resulting in etio-chloroplasts, and then, within a few hours, in fully functional chloroplasts (Kowalewska et al., 2019; Solymosi & Aronsson, 2013). The etioplast-to-chloroplast transition is part of the so-called de-etiolation process also under natural conditions (Solymosi & Schoefs, 2010) and coincides with greening due to the onset of Chl biosynthesis (Solymosi & Aronsson, 2013).

Greening can be easily followed by spectroscopic methods because the delocalized electron clouds of the porphyrin rings of Pchlide, Chlide and Chl are very sensitive to the molecular micro-environment of the chromophore; the spectral properties of the pigment can then indicate the smallest changes associated with its organization or environment. Pigment molecules in similar molecular environments have similar emission properties and are referred to as pigment forms, designated below by their fluorescence emission maxima at 77 K temperature. Pchlide with emission at 633 nm is located in the PTs or the plastid envelope and is not photoactive as it is not bound to the active site of POR (Böddi et al., 1992). Pchlide pigments bound to dimers or oligomers of POR in the PLBs have fluorescence emission maximum at 655 nm, and are referred to as photoactive Pchlide, as they can readily be transformed into Chlide with emission maximum at 690 nm upon illumination. When samples are kept at room temperature after illumination for approx. 30 minutes, the oligomers of Chlide-POR undergo disaggregation, resulting in a spectral blue shift of the fluorescence emission maximum towards 680 nm called Shibata shift (Smeller et al., 2003). After this shift, Chlide is dissociated from POR, gets esterified and is gradually built into the Chl-protein complexes of the photosynthetic apparatus. For instance, after 2–4 hours of greening, a Chl form with fluorescence at 684 nm is detected (Franck et al., 1997). In green and greening leaves, fluorescence emission bands at 685, 695, 720 and 735–740 nm appear, which belong to the PSII reaction centre and CP43, CP47 of PSII, PSI core complexes, and PSI-LHCI complexes, respectively (Kalaji et al., 2017). The effect of soil salinity on greening is an important factor from the agricultural point of view because many important crops (like wheat) are sown at 5–10 cm depth in the soil according to agricultural protocols. Thus, wheat seedlings develop in the dark within the soil for several days, become etiolated and their leaf tip gets exposed to light gradually as the seedling reaches the soil surface. In this agricultural context, it is interesting to study how etioplasts, different etio-chloroplasts and chloroplasts react to the same type of salt stress treatment.

Salinity inhibits crop germination, growth and yield, and thus represents a major threat to agricultural productivity (Shrivastava & Kumar, 2015). Salinity influences plant metabolism in a complex manner, including, among others, the indirect effects of salt-induced osmotic stress. However, the accumulation of salt within cells may also disrupt several processes of plant metabolism, resulting in negative physiological alterations in plants, such as decrease in photosynthesis (Ounoki et al., 2021), and in ultrastructural changes (Hameed et al., 2021). Ultrastructural data in the literature are somewhat controversial: some authors observed the swelling of the thylakoid lumen in chloroplasts (Hasan et al., 2006; Ounoki et al., 2021; Rahman et al., 2000), while others do not report any alterations in plastid structure under salt stress (Hasan et al., 2006; Ounoki et al., 2021). However, even within the same species, depending on the type or length of treatment (Ounoki et al., 2021) or the studied cell type (Hasan et al., 2006), plastid structure was either affected or not affected by salt stress. Also, the molecular background of these alterations is still unclear. Data about other plastid types, like etioplasts of dark-grown seedlings, have shown either no effect (Mitsuya et al., 2000) or swelling of the PT lumen (Abdelkader et al., 2007a) and strong inhibition of Chl biosynthesis (Abdelkader et al., 2007a, 2007b; Turan and Tripathy, 2015). The relationship between the swelling of the lumen, the changes in plastid metabolism (including photosynthesis), and the effect of light on these processes are also not well established. Salinity is often linked to oxidative stress due to the formation of reactive oxygen species (ROS), especially under light conditions (Mitsuya et al., 2003a; Yamane et al., 2004). The (pro)thylakoids of etioplasts were highly sensitive to salt shock treatment (600 mM NaCl:KCl, 1:1) (Abdelkader et al., 2007a). The applied salt concentration equals that of seawater and has natural relevance in case of tsunamis or strong seawater seepage in coastal agricultural areas with wheat seedlings developing in the soil.

In this work, we wanted to check whether swelling was induced by the osmotic or ionic component of the salt shock treatment by comparing the effects of the above salt solution with isosmotic polyethylene glycol (PEG) solution. We also investigated whether the same salt treatment induced similar ultrastructural alterations in chloroplasts or in etio-chloroplasts at different stages of greening to understand which greening stage is more sensitive to salinity-induced ultrastructural and functional alterations.

2 | MATERIALS AND METHODS

2.1 | Plant material and experimental design

Wheat (*Triticum aestivum* L. cv. Mv Béres) seeds were obtained from the Agricultural Institute, Center for Agricultural Research (Martonvásár, Hungary). Seeds were germinated for 11 days at room temperature (22°C) either in the dark to become fully etiolated or in light (100 µmol photons m^{-2} s^{-1} photon flux density [PFD], white light, for 12 h/12 h light–dark cycles) to become fully light-grown, green seedlings (see Figure 1). In addition to dark-grown seedlings used directly for the experiments, some intact dark-grown plants were exposed to light for greening for 2, 4 or 16 h under continuous light of 50 µmol photons m^{-2} s^{-1} PFD and then used for treatments and analyses (Figure 1).

For all treatments, the oldest, initial 1-cm-long leaf tip of the first leaf was discarded and the next 2-cm-long leaf segment was used. The leaf segments were floated either on 1/2 Hoagland solution

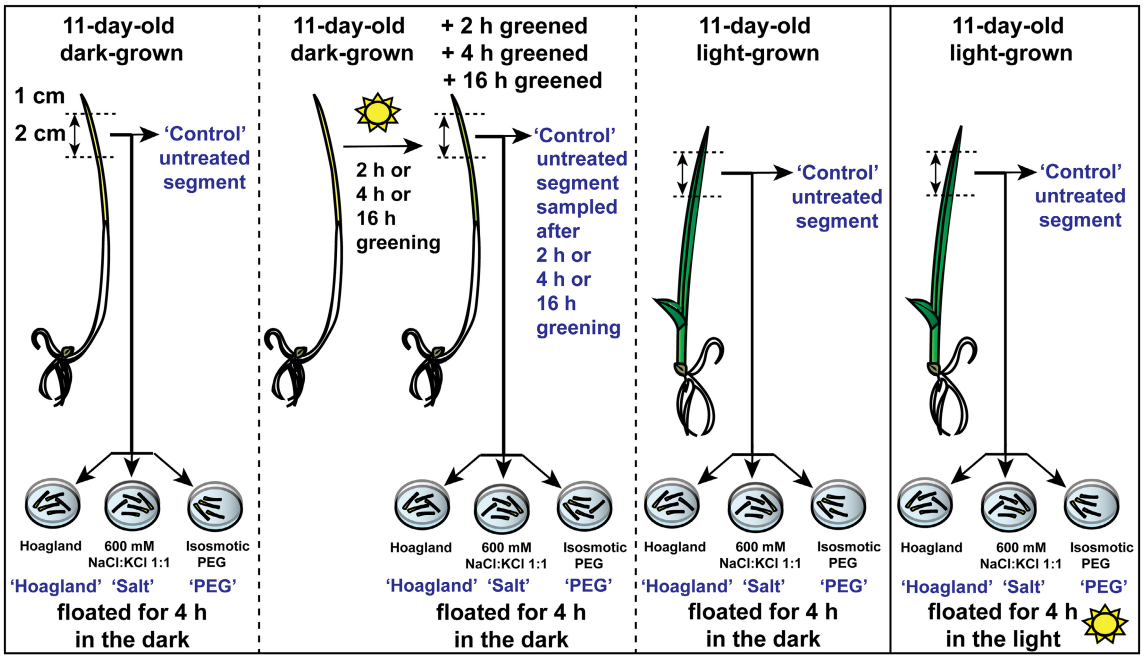

FIGURE 1 Outline of the used plant material, applied light regimes, and treatments as described in the manuscript.

(Hoagland & Arnon, 1950) or on 600 mM salt (NaCl:KCl, 1:1 dissolved in Hoagland, referred as 'Salt') or on isosmotic solution of PEG 6000 (dissolved in Hoagland, referred to as 'PEG') in Petri dishes for 4 h either in the dark or, in case of the light-grown plants, also under continuous light (250 µmol photons m^{-2} s^{-1}). For comparison, in some cases, leaf segments without floating on the above solutions were also added and will be referred to as 'Control' in the manuscript (see Figure 1). The osmolarity of the 600 mM NaCl:KCl (1:1) solution was 1054 mOsm as measured with a Gonotec Osmomat 3000 osmometer. Therefore, the PEG solution was prepared to have a final osmolarity of the same value (1054 mOsm).

2.2 | Leaf relative chlorophyll content

The relative Chl content of the leaf segments was measured using a portable soil plant analysis development (SPAD) meter (Konica Minolta SPAD-502^{+} Chlorophyll Meter®). For each treatment, measurements were performed on at least 10 separate segments (each from a different plant). Three data points were measured in different regions of each leaf segment, and the experiments were done in 3–5 independent repetitions. For other analyses, Chl was extracted from leaf disks or thylakoids, centrifuged and then spectrophotometrically quantified as in Porra et al. (1989).

2.3 | Fluorescence spectroscopy at 77 K

Plant leaf segments were placed in glass tubes and submerged in liquid nitrogen. The 77 K fluorescence spectroscopic measurements and subsequent correction of the spectra were performed as in Ounoki et al. (2021) using FluoroMax-3 spectrofluorometer (Jobin-Yvon Horiba) and SPSERV V3.14 software (copyright: C. Bagyinka, Biological Research Center, Hungary). At least 3 independent experiments were carried out, and at least 3 different plants were sampled in each experiment ($n = 9–29$). The spectra were first normalized to their maxima to compensate for potential size, shape, and geometrical variances of the measured leaf segments. Normalized spectra were then averaged and are shown for the different treatments. We also performed statistical analyses to compare the relative fluorescence emission maximum values of each major peak in the spectra recorded for the various samples.

2.4 | Thylakoid isolation and 2D Blue Native/SDS PAGE

The plastids were isolated under dim laboratory light after having removed the treatment solutions from the leaf pieces by washing them with distilled water in a Nutch filter. For isolation of plastids, leaves were homogenized in isolating buffer (50 mM 4-(2-hydroxyethyl)-1-piperazineethanesulphonic acid (HEPES)-KOH, pH 7.0, 330 mM sorbitol, 2 mM ethylenediaminetetraacetic acid (EDTA), 2 mM $MgCl_2$, 0.1% (w/v) bovine serum albumin (BSA), 0.1% (w/v) Na-ascorbate) at 4°C for 3 x 3 s by Waring Blender. After filtration, chloroplasts or etiochoroplasts were immediately centrifuged in a swing-out rotor (1000/3000 × *g*, 5 min, 4°C), and washed in isolating buffer without BSA and Na-ascorbate. Isolation and washing of thylakoid membranes (osmotic shock and washing out part of the coupling factor 1) was carried out as in Sárvári et al. (2022). Light-grown, 16 h greened and 4 h

greened thylakoids (500, 500, and 20 μg Chl ml^{-1}) were solubilized with 1%, 1% and 2% (w/v) n-dodecyl-β-D-maltoside (β-DM, SIGMA), respectively, plus 1% digitonin (SERVA) on ice for 30 min. The supernatant obtained after centrifugation (18,000 × *g* for 15 min at 4°C) was supplemented with 1/5 volume of 5% (w/v) Serva Blue G dissolved in 500 mM aminocaproic acid, and 10–15 μL of the solubilized material was applied per lanes. For the separation of thylakoid complexes, Blue Native polyacrylamide gel electrophoresis (BN PAGE), subsequently second dimension SDS-PAGE and densitometric analyses of the gels were performed as described in Sárvári et al. (2022). BN patterns of 4 h greened samples were stained using the Blue-Silver method (Candiano et al., 2004). Exact parameters of gel electrophoresis are mentioned in the Figure legends. The identity of the complexes was recognized as in Basa et al. (2014). Data represent means and standard deviations of values obtained from at least two independent experiments with 2–4 technical replicates (n = 4–9).

2.5 | Measurement of photosynthetic activity

FluorPen FP 100 (Photon Systems Instruments) instrument was used to evaluate the photosynthetic parameters. Chl *a* fluorescence induction kinetics were recorded in light-adapted and 20-min dark-adapted samples to calculate "Qy light" (equivalent to F_v'/F_m') and "Qy dark" (corresponding to F_v/F_m), respectively. These parameters characterize the photochemical activity and structural dynamics of photosystem II (PSII) in the light- and dark-adapted samples, respectively (Björkman & Demmig, 1987; Sipka et al., 2021). For each treatment, measurements were performed on at least 4–5 separate segments, and at least 3 independent experiments were carried out.

2.6 | Transmission electron microscopy

Leaf sections (1 mm × 1 mm) were cut from the middle of treated leaf segments. These sections were fixed, dehydrated, embedded, sectioned, stained and analyzed by transmission electron microscopy (TEM) as described in Ounoki et al. (2021). Ultrathin (70 nm) sections were investigated using a JEOL JEM 1011 transmission electron microscope (JEOL Ltd.) at an accelerating voltage of 80 kV. Digital photographs of typical plastid sections captured using an Olympus Morada CCD camera are shown. To identify the granum thylakoid membrane repeat distance values on TEM micrographs, ImageJ (NIH; Schneider et al., 2012) software was used to conduct a fast Fourier transformation (FFT) on the specified region of interest (i.e., grana) of the micrographs as in Ounoki et al. (2021). Several (51–131) grana from 25–35 randomly taken plastid sections per treatment were analyzed and averaged.

2.7 | Small-angle neutron scattering

Small-angle neutron scattering (SANS) measurements were performed using the Yellow Submarine instrument at the Budapest Neutron Center, Hungary (Almásy, 2021). To cover the range of scattering vector (*q*) from 0.016 to 0.06 $Å^{-1}$, 5.3 m sample-to-detector distance and 6.13 Å wavelength was used. The treated and control leaf segments (4–6 pieces) were placed in Hellma quartz cuvettes of 2 mm path length filled with D_2O-containing Hoagland solution with and without 600 mM NaCl:KCl (1:1). Therefore, each SANS scattering profile represents the statistical average of 4–6 leaf segments.

The raw data were treated with the BerSANS program (Keiderling, 2002). Raw data were normalized to the number of beam monitor counts and corrected for detector efficiency; instrumental background and scattering from the solution were subtracted from the scattering profiles. 360° radial averaging was performed to reduce the obtained 2D profiles to 1D, which were then fitted by the linear combination of a constant, a power and a Gauss function in the *q* range of 0.016–0.046 $Å^{-1}$. The repeat distance ($RD = 2\pi/q^*$, where q^* is the center position of the Bragg peak) of granum thylakoids represents the sum of the thickness of the two membrane layers, and the width of the two aqueous phases, the lumen and the interthylakoidal space (Füzi et al., 2017; Nagy & Garab, 2021; Ünnep et al., 2014). Three independent biological replicates were measured, and typical scattering profiles are shown for each treatment.

2.8 | Malondialdehyde measurement

Malondialdehyde (MDA) levels of differently treated leaves can be used to determine the degree of lipid peroxidation (Parihar et al., 2015). To this aim, 100 mg of leaf samples were homogenized in 1 mL of 0.1 (w/v) trichloroacetic acid and centrifuged at 15,000 × *g* for 15 min. Equal parts of 0.5% (w/v) thiobarbiturate and 20% (v/v) trichloroacetic acid were added to the supernatant. After incubation of the mixtures at 90°C for 30 min, the MDA concentration was determined by recording the absorbance at 532 nm and using the following extinction coefficient: $\varepsilon = 155\ mM^{-1}\ cm^{-1}$. Light scattering was corrected based on the increase in the extinction in the 800 to 730 nm region. For each treatment, measurements were performed in 3–4 technical replicates in at least 3 different experiments.

2.9 | High-temperature thermoluminescence measurements

Thermoluminescence (TL) measurements were performed using a home-built set-up similar to the one used by Podmaniczki et al. (2021) with extended temperature range. TL is a technique that consists of a rapid cooling of a sample followed by its progressive warming to thermally induce photon emission and reveal temperature-dependent emission bands due to different types of charge pairs (with pre-illumination) and high-temperature TL (HTTL) due to the radiative thermolysis of peroxides (without pre-illumination) (Ducruet & Vavilin, 1999). The measurements were controlled and recorded by using a National Instrument data acquisition device via custom-designed LabVIEW software. The leaf samples, preadapted to darkness for 5 min in the sample chamber, were heated from 20 to 160°C at a rate of 30°C min^{-1}, during which the high-temperature glow curves were recorded.

3–4 leaf segments were measured in the sample holder at once, 3 different measurements were performed per experiment and treatment. Experiments were repeated independently three times. Images show the average of three independent measurements in one treatment. Curves were normalized to their integrated intensity using OriginPro Software (OriginLab Corporation).

2.10 | Statistical analyses

Normality test, t-test in case of SANS data, one-way ANOVA or, in case of samples not following normal distribution, Kruskal-Wallis nonparametric ANOVA, and if necessary adequate post hoc tests, Tukey–Kramer or Dunn's multiple comparisons were performed using GraphPad Prism 8 (GraphPad Software) as described in Ounoki et al. (2021). In the Figures and Tables, different letters indicate significant differences ($P < 0.05$). Unless otherwise stated, standard deviations of the data are shown in the Figures, while Tables contain mean values with standard errors.

3 | RESULTS

3.1 | Leaf relative chlorophyll content (SPAD)

First, SPAD values referring to relative Chl content and Qy values representing the photosynthetic activity, as general parameters characterizing the developmental stage of plastid membranes, were analyzed (Table S1).

The SPAD measurements revealed significantly decreased values in all salt-treated segments (Figure 2, Table S1). The reduction of SPAD index values of light-grown leaf segments was higher in the light than in the dark salt treatment (control values decreased by 41% and by 15%, respectively; see Figure 2A, B). The salt-induced reduction in the SPAD values was higher in less greened leaf segments; i.e. SPAD value decreased by 66% after 16 h of light (Figure 2C), while it decreased by 60% after 4 h light (Figure 2D) when compared with the control. Osmotic stress induced by PEG also resulted in a significant, although lower, decrease in the SPAD index values in the 16-h and 4-h greened samples and the light-grown plants' segments treated with PEG in the dark for 4 h (Figure 2B-D). Dark-grown leaves contained no Chl, and the Chl(ide) contents of the dark-grown plants greened for 2 h were also very low; therefore, their SPAD index values could not be determined.

3.2 | Fluorescence emission of pigment-protein complexes at 77 K

To characterize the stage of Chl biosynthesis and the interactions of the photosystems in the photosynthetic apparatus, 77 K fluorescence emission spectra were recorded, corrected, normalized and averaged (Figure 3).

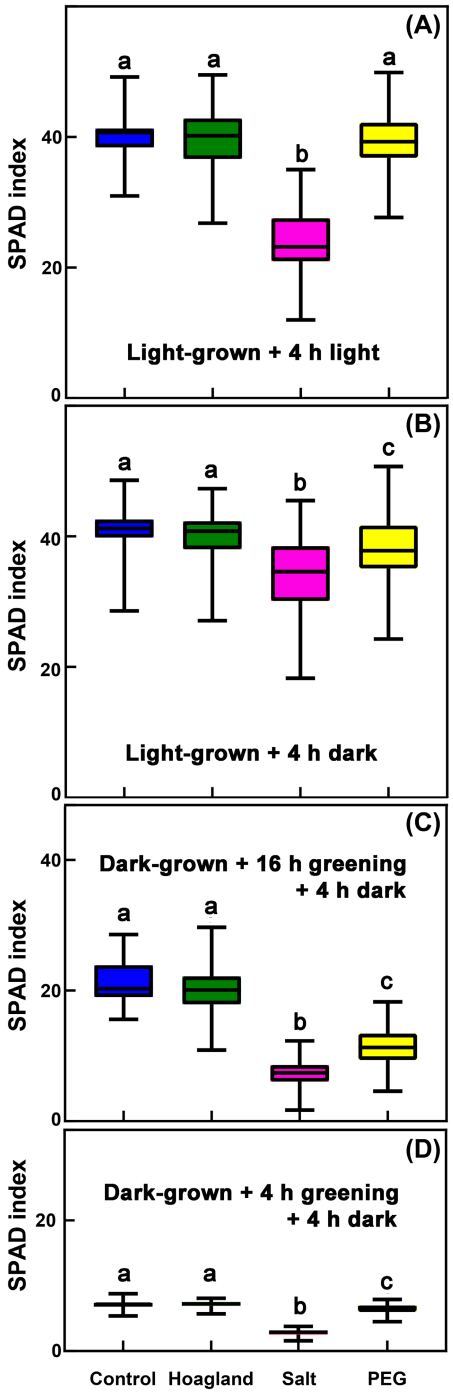

FIGURE 2 (A-B) SPAD index values of light-grown wheat leaf segments floated for 4 h in the light (A) or in the dark (B) on Hoagland solution ('Hoagland'), 600 mM NaCl:KCl (1:1) solution ('Salt') or isosmotic polyethylene glycol (PEG-6000, 'PEG') solution; and (C-D) intact dark-grown seedlings first greened for 16 h (C) or 4 h (D) on continuous light and then treated for 4 h in the dark on the same solutions. 'Control' refers to respective samples without any floating. For each treatment, measurements were performed on at least 10 segments from 10 different plants. Data were recorded at the top, middle and lowermost part of each segment, and measurements were performed in 3–5 independent repetitions. Different letters indicate statistically significant differences between the means of the samples according to Kruskal-Wallis nonparametric ANOVA followed by Dunn's multiple comparisons post hoc test ($P < 0.05$) ($n = 90–249$).

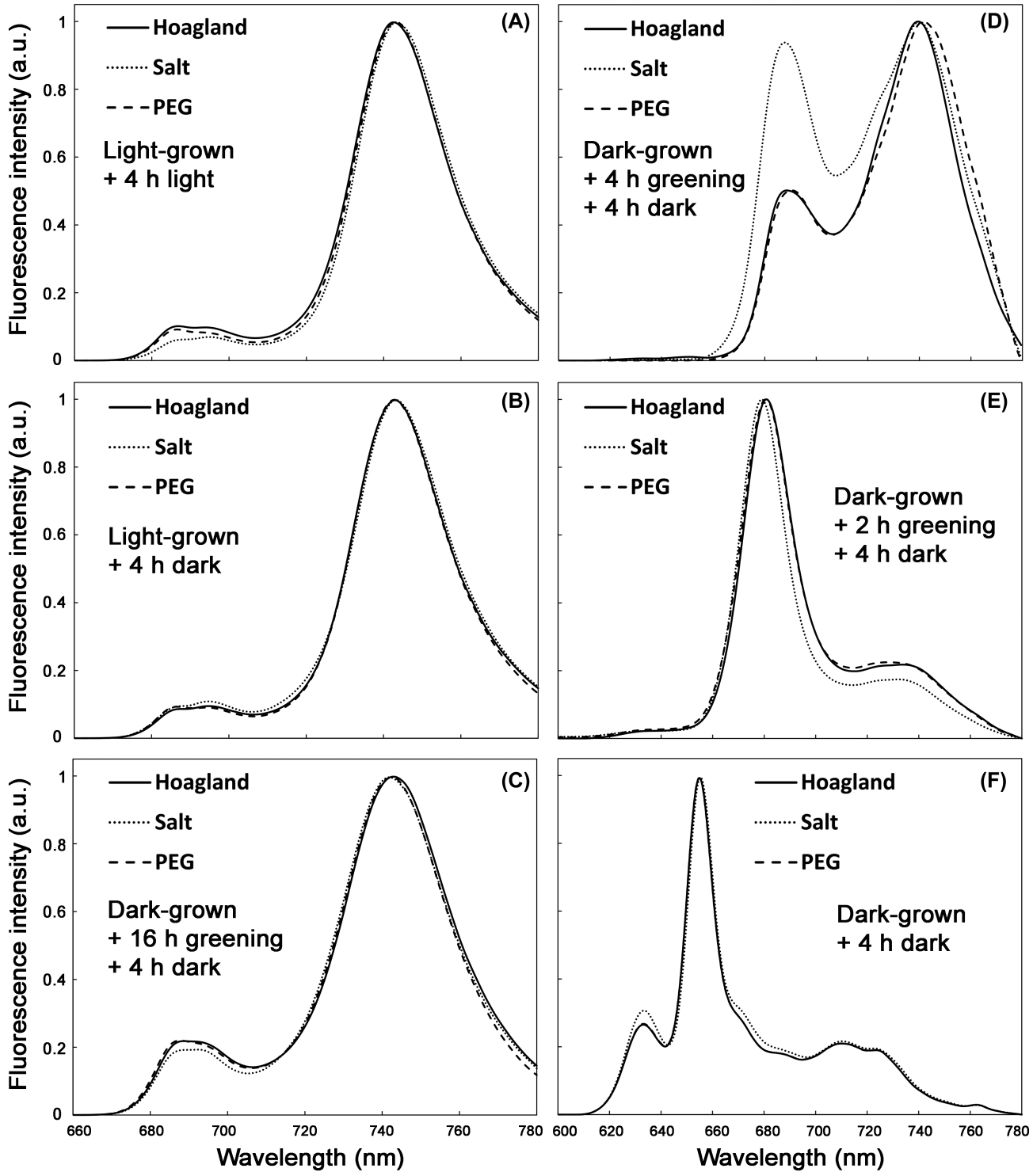

FIGURE 3 77 K fluorescence emission spectra of wheat leaf segments floated for 4 h in the light (A) or in the dark (B-F) on Hoagland solution ('Hoagland'), 600 mM NaCl:KCl (1:1) solution ('Salt') or isosmotic polyethylene glycol (PEG-6000, 'PEG') solution. (A, B) Leaf segments of light-grown seedlings. (C-F) Leaf segments of intact dark-grown seedlings greened for 16 h (C), 4 h (D), 2 h (E) and 0 h (F) on continuous light and then treated for 4 h in the dark on the same solutions. Spectra (n = 9–29, at least 3 independent experiments were carried out, with at least 3 independent repetitions, i.e., at least three different plants per treatment) were corrected, normalized to their maxima, and then averaged.

In light-grown leaves, the fluorescence spectra are mainly characterized by three Chl emission peaks, located at around 685 and 695 nm (red peaks) and at around 740–750 nm (far-red peak). In the light-grown wheat leaf segments treated for 4 h in Hoagland, salt or PEG solutions in the light, a slight decrease in the relative intensity of the short-wavelength 685 nm and 695 nm emission bands was

observed under salt stress (Figure 3A), whilst no changes were observed when the treatments were performed in the dark (Figure 3B). If the spectra were normalized to the short-wavelength maximum, a clear increase in the PSI fluorescence emission was observed in the spectra of green leaves treated for 4 h in the light with PEG and especially with salt.

In the case of treatments performed after 16 h greening, the fluorescence emission spectra of the leaves were almost identical to those of light-grown leaves (Figure 3C). A very slight difference was found in the salt-floated samples when treated in light: the relative fluorescence intensity of the 685 and 695 nm bands decreased slightly, but significantly, when compared with the spectra of Hoagland or PEG-treated leaves.

In the dark-grown wheat leaf samples, the short-wavelength fluorescence emission bands at 633 and 655 nm (corresponding to Pchlide-protein complexes) were only detected, and we observed a very slight, statistically not significant increase in the relative intensity of the short-wavelength Pchlide form at 633 nm in the salt-treated segments (Figure 3F). When dark-grown leaf segments were greened for 2 h before being treated in the dark for 4 h, the fluorescence emission spectra in the Hoagland, salt and PEG solutions exhibited maxima at 681, 679 and 680.5 nm, respectively. In addition to the Chl(ide) emission band, indicating the successful phototransformation of the photoactive Pchlide form and the subsequent Shibata shift, the weak fluorescence emission band at 633 nm indicated some residual non-photoactive Pchlide in the samples (Figure 3E). In the samples floated on salt, the relative fluorescence emission maximum around 730–740 nm was significantly lower than in the other two samples.

After longer – 4 h – greening and subsequent treatments on the same solutions in the dark for 4 h, the relative intensity of the short-wavelength fluorescence emission bands at 633 and 650 nm (corresponding to Pchlide-protein complexes) became almost undetectable, and fluorescence emission spectra indicated more or less developed photosynthetic apparatus, with long-wavelength fluorescence bands corresponding to Chl-protein complexes at around 690 and 740 nm, which became dominating. After 4 h greening (and the subsequent 4 h treatment in the dark), samples floating on Hoagland or PEG had similar appearance, resembling the spectra of light-grown leaves, whilst the 689 and 740 nm bands (the latter with a 720 nm shoulder) had similar height in samples floating on salt, indicating somewhat hindered greening, i.e. the presence of more PSI core complexes fluorescing at 720 nm (Lamb et al., 2018) and less organized PSII in these samples (Figure 3D).

3.3 | Alterations in the chlorophyll-protein complex pattern

The BN PAGE patterns of light-grown or 16-h-greened wheat thylakoids isolated from leaf segments floated on Hoagland, salt or PEG solution resulted in 11 clear bands (Figure 4A). Based on their polypeptide patterns (Figure S1, see also Basa et al. 2014), they were identified as megacomplexes (different PSI and PSI-PSII-LHCII megacomplexes) in agreement with literature data (Grieco et al., 2015; Järvi et al., 2011; Yokono et al., 2015, 2019), PSI (PSI-LHCII, PSI), PSII (PSII-supercomplexes, dimers and monomers), light-harvesting complexes (LHCII-assembly: CP29-CP24-LHCII-t, LHCII-trimer and Lhc-monomers), cytochrome (Cyt) b_6/f complex in dimeric form, and ATP synthase complexes (ATPs - running in the PSI band and coupling factor1 running near to PSII monomer). Thylakoids isolated from the 4-h-greened leaf segments, which contained low amount of Chl (about 54.3 ± 27.2 μg Chl g^{-1} FW compared to the light-grown control having 2310.7 ± 229.0 μg Chl g^{-1} FW), showed the presence of only PSI and PSII monomers, some LHCII-trimer, dimeric Cyt b_6/f complexes and the different assembly forms of ATPs (Figure S2).

Floating and 4 h treatments of green or 16-h-greened leaf segments did not significantly alter the whole thylakoid composition. Nevertheless, some changes in the organization of complexes were detected. In light-grown leaf segments, the PEG treatment only increased the amount of PSI-LHCII both in the light and in the dark (Figure 4B, C). However, remarkable reorganization of PSII was observed under salt treatment: disassembly of some megacomplexes and PSII supercomplexes (PSII-s) increased the amounts of PSII-dimers, monomers, LHCII assembly complex, and Lhc monomers.

In the thylakoids isolated from the 16-h-greened and then 4 h dark salt-treated leaf segments, only the amount of PSII monomer decreased significantly (Figure 4D). Due to the low amount of Chl, the complexes in 4-h-greened 4 h dark-floated leaf segments could not be quantified properly.

3.4 | Photosynthetic activity

The Qy dark (Fv/Fm, Figure 5) and Qy light values (Fv′/Fm′, Figure 6) characterizing photochemical activity and structural dynamics of PSII (Sipka et al., 2021) were determined in 20 min dark-adapted or in light-adapted leaf segments, respectively (see also Table S1).

While the control plants (plants without floating) and plants floated on Hoagland showed similar Qy dark and Qy light values (Figures 5 and 6), these parameters decreased significantly in all salt-treated samples. Qy dark values decreased both in the light-grown wheat leaf samples floating 4 h in the light (by 16% compared to their control values) and in the dark (only by 4%) on salt solution (Figure 5A, B) and also in 4-h (by 60%) and 16-h-greened (by 20%) dark-grown leaves subsequently salt-treated for 4 h in the dark (Figures 5C, D). Similarly to Qy dark results, the Qy light values also decreased significantly in all salt-treated samples by 28% and 8%, respectively, in light-grown samples treated in the light or in the dark, and by 21% and 75% in dark-grown and 16-h and 4-h-greened samples treated in the dark, with the largest decrease observed after 4 h greening (Figure 6A-D).

In dark-grown samples and 2-h-greened dark-grown samples, no PSII activity could be observed. The activity first appeared after 4 h greening, but its value was very low (Figures 5D and 6D).

PEG treatment only induced a significant decrease in the Qy dark and Qy light values in the case of light-grown plants treated for 4 h in

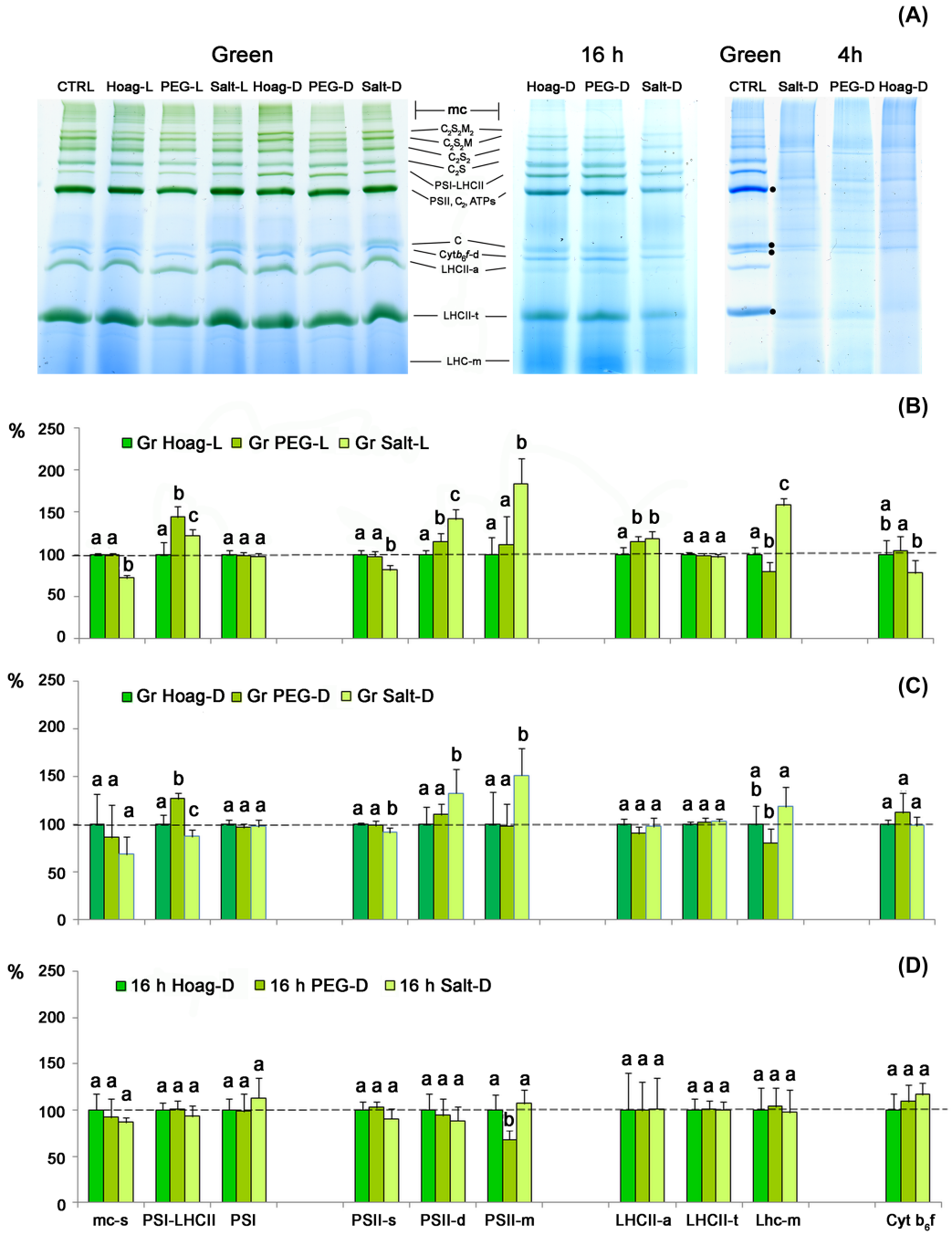

FIGURE 4 Changes in the organization of thylakoid complexes in differently treated wheat leaf segments. (A) Chl-protein bands separated in 4.3–12% BN gel gradient. The dark-grown and then 4-h-greened and then 4 h dark-treated samples were Coomassie-stained after the separation. Pieces of light-grown ('green'), dark-grown then 16-h ('16 h') and 4-h-greened ('4 h') leaves were floated on Hoagland ('Hoag') or 600 mM KCl:NaCl (1:1) ('Salt') or isosmotic polyethylene glycol (PEG-6000, 'PEG') solutions either in the light ('L') or in darkness ('D') for 4 h. 'CTRL' refers to thylakoids isolated from untreated intact light-grown wheat leaf segments of the same age. Light-grown (5.3 ± 0.5 μg protein μg^{-1} Chl) and 16-h-greened thylakoids (6.4 ± 0.9 μg protein μg^{-1} Chl) were solubilized using 1% β-DM plus 1% digitonin at 500 μg Chl ml^{-1} sample concentration, while 4-h-greened thylakoids (139.0 ± 81.3 μg protein μg^{-1} Chl) were solubilized using 2% β-DM plus 1% digitonin at 20 μg Chl ml^{-1} sample concentration. PS – photosystem, LHC – light-harvesting complex, LHCII-a – LHCII-assembly: CP29-CP24-LHCII-t, C – core complex of PSII, S and M – LHCII trimers attached to the PSII core strongly and moderately, mc-s – megacomplexes, t – trimer, m – monomer, Cyt b_6f – cytochrome b_6/f complex, ATPs – ATP synthase. (B, C, D) Relative amounts of complexes (determined in pixel density in lanes supplied with the same amount of Chl and expressed as the percentage of the samples floated on Hoagland solution) in thylakoids isolated from light-grown, green (Gr) seedlings treated in the light (B) or in the dark (C), and from 16-h-greened dark-grown seedlings treated in the dark (D) for 4 h. PSII-s – supercomplexes of PSII core complexes (C) with LHCII trimers (S and M), PSII-d – C_2, PSII-m – C. Different letters indicate statistically significant differences between the means of samples (from at least two independent experiments with 2–4 technical replicates, n = 4–9) according to Kruskal-Wallis nonparametric ANOVA followed by Dunn's multiple comparisons post hoc test ($P < 0.05$).

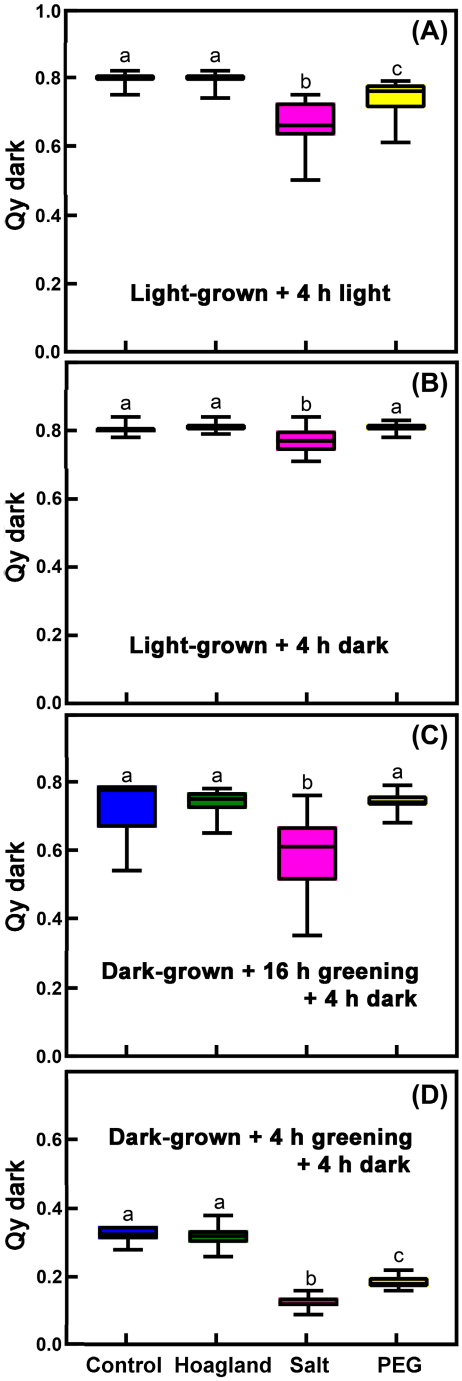

FIGURE 5 Variations of the Qy dark PSII fluorescence parameter of wheat leaf segments floated for 4 h in the light (A) or in the dark (B-D) on Hoagland solution ('Hoagland'), 600 mM NaCl:KCl (1:1) solution ('Salt') or isosmotic polyethylene glycol (PEG-6000, 'PEG') solution. 'Control', refers to respective leaf segments collected without any floating from intact light-grown plants (A, B) or from intact dark-grown seedlings first greened for 16 h (C) or 4 h (D) on continuous light. For each treatment, measurements were performed on at least 4–5 separate segments, and at least 3 independent experiments were carried out (n = 20–31). Different letters indicate statistically significant differences between the samples according to Kruskal-Wallis nonparametric ANOVA followed by Dunn's multiple comparisons post hoc test ($P < 0.05$).

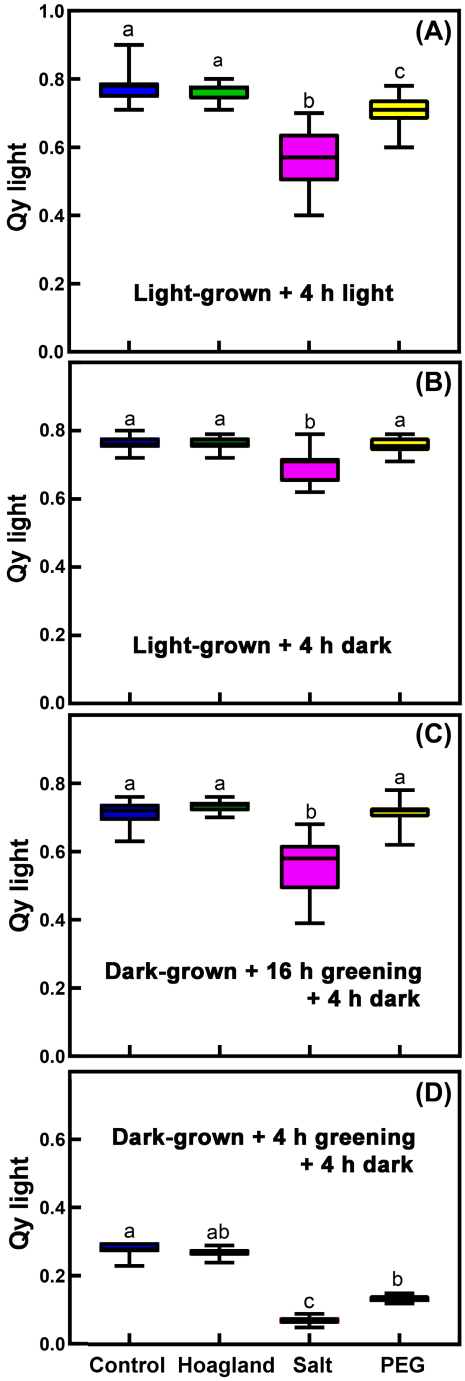

FIGURE 6 Variations of the Qy light PSII fluorescence parameter of wheat leaf segments floated for 4 h in the light (A) or in the dark (B-D) on Hoagland solution ('Hoagland'), 600 mM NaCl:KCl (1:1) solution ('Salt') or isosmotic polyethylene glycol (PEG-6000, 'PEG') solution. 'Control', refers to respective leaf segments collected without any floating from intact light-grown plants (A, B) or from intact dark-grown seedlings first greened for 16 h (C) or 4 h (D) on continuous light. For each treatment, measurements were performed on at least 4–5 separate segments, and at least 3 independent experiments were carried out (n = 13–34). Different letters indicate statistically significant differences between the samples according to Kruskal-Wallis nonparametric ANOVA followed by Dunn's multiple comparisons post hoc test ($P < 0.05$).

the light as well as in the plants in the very early phase of greening (dark-grown leaves greened for 4 h and then treated for 4 h in the dark) (Figures 5A, D and 6A, D).

3.5 | Changes observed in plastid ultrastructure

No important differences were observed between the control leaf segments floated on Hoagland and the plants floated on PEG (Figure 7A, C). The plastid sections in these samples sometimes contained small vesicles (e.g., Figure 7A).

In dark-grown wheat leaf segments floating on salt solution in the dark for 4 h, we found swelling of the PT lumen and the appearance of envelope invaginations in the etioplasts (Figure 7B) similar to data in Abdelkader et al. (2007a). The studied plastid sections also contained sometimes spotted bodies (e.g., Figure 7B), typical for etiolated wheat and reported in the literature as microtubule-like structures insensitive to microtubule inhibitors (Artus et al., 1990).

Ultrastructural analyses of light-grown wheat leaf segments showed no important differences after 4 h of dark treatment on the different solutions (Figure 7D-F). Envelope invaginations and vesicles sometimes appeared in the salt-stressed leaves. When the same salt stress was applied for 4 h in the light, no swelling was visible in the chloroplasts (Figure 7G-I), but all quantitative parameters of granum size significantly decreased (Table 1) when compared to the sample floated on Hoagland.

In PEG-treated wheat leaf segments, the orientation of the thylakoid system became somewhat disordered during 4 h in the light (compare Figure 7G and I), but this was not accompanied by any quantitative changes in granum morphology (Table 1).

To confirm the shrinkage of thylakoid membranes, we conducted SANS measurements on the salt-stressed leaves. This non-invasive method provides statistically averaged information about the

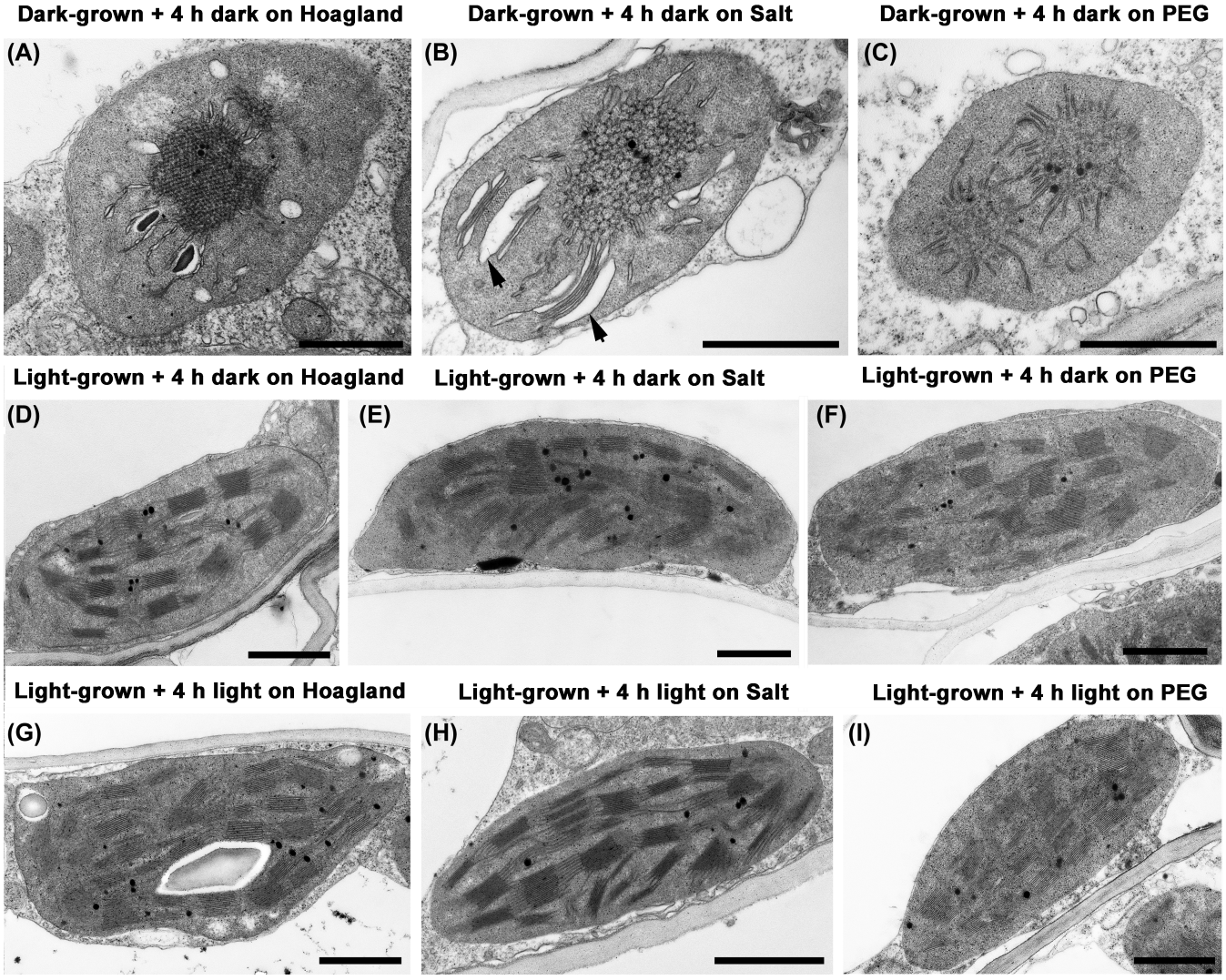

FIGURE 7 Transmission electron micrographs of typical plastid sections of dark-grown (A-C) or light-grown (D-I) wheat leaf segments floated for 4 h in the dark (A-F) or in the light (G-I) on Hoagland solution ('Hoagland') (A, D, G), 600 mM NaCl:KCl (1:1) solution ('Salt') (B, E, H) or isosmotic polyethylene glycol (PEG-6000, 'PEG') solution (C, F, I). Black arrow: swollen prothylakoid. Scale bar: 1 μm.

TABLE 1 Means and standard error values of granum parameters of the chloroplasts of light-grown wheat leaf segments floated for 4 h in the light or in the dark on Hoagland solution ('Hoagland'), 600 mM NaCl:KCl (1:1) solution ('Salt') or isosmotic polyethylene glycol (PEG-6000, 'PEG') solution; and of intact dark-grown seedlings first greened for 16 h on continuous light and then treated for 4 h in the dark on the same solutions. Several (51–131) grana from 25–35 randomly taken plastid sections per treatment were analyzed and averaged (n = 51–131). Different letters indicate statistically significant differences between the samples according to Kruskal-Wallis nonparametric ANOVA followed by Dunn's multiple comparisons post hoc test ($P < 0.05$)

	Granum height (nm)	Number of thylakoids/granum	Granum diameter (nm)	Repeat distance (nm)
Light-grown wheat leaf segments floated for 4 h in the dark				
Hoagland (n = 91)	254 ± 11[a]	13 ± 1[a]	415 ± 9[a]	18.7 ± 0.2[a]
Salt (n = 131)	248 ± 11[a]	13 ± 0[a]	397 ± 6[a]	19.4 ± 0.2[a]
PEG (n = 115)	274 ± 12[a]	14 ± 1[a]	406 ± 8[a]	19.0 ± 0.2[a]
Light-grown wheat leaf segments floated for 4 h in the light				
Hoagland (n = 75)	251 ± 8[a]	14 ± 0[a]	413 ± 7[a]	18.6 ± 0.1[a]
Salt (n = 88)	163 ± 5[b]	11 ± 0[b]	356 ± 5[b]	15.5 ± 0.3[b]
PEG (n = 51)	293 ± 11[a]	15 ± 1[a]	399 ± 8[a]	19.1 ± 0.2[a]
Leaf segments of 16 h greened intact wheat seedling floated for 4 h in the dark				
Hoagland (n = 57)	76 ± 4[a]	3 ± 0[a]	476 ± 13[a]	19.4 ± 0.3[a]
Salt (n = 55)	43 ± 2[b]	2 ± 0[b]	296 ± 9[b]	16.1 ± 0.2[b]
PEG (n = 75)	80 ± 4[a]	3 ± 0[a]	410 ± 9[c]	20.6 ± 0.2[c]

multilamellar thylakoid membrane system of chloroplasts, the so-called grana, and their periodic organization (i.e., repeat distance value, RD) *in vivo*, for all grana present in all chloroplasts of the leaves in the neutron beam.

Salt treatment of light-grown leaf segments for 4 h in the light led to a well-discernible shrinkage of granum thylakoid membranes (Figure 8). This is reflected by the decreased RD values from 212 ± 3 Å (n = 3) in Hoagland to 179 ± 4 Å (n = 3) in salt solution. The obtained RD data using SANS (Figure 8) or TEM data of the same plant material (Table 1) are in good agreement (showing decreased RD values in samples treated with salt in the light), although the RD values obtained by TEM are always smaller than RD values obtained by SANS. This discrepancy can be explained by possible artefacts resulting from fixation and dehydration of the TEM samples prior to analyses (Ünnep et al., 2014).

After having seen that only etioplasts show the typical salt stress-induced specific swelling of the (pro)thylakoid lumen under our experimental conditions, and fully developed chloroplasts do not have similar ultrastructural alteration, we decided to investigate the effect of salt stress on the structure of young etio-chloroplasts at different stages of greening. First, we checked what happened if we greened intact dark-grown plants for 16 h under low light conditions (50 µmol photons m^{-2} s^{-1}) and then had their 2-cm-long upper segments floated on Hoagland solution in the dark for 4 h (Figures 1 and 9A). We observed young, elongated chloroplasts with developing grana containing 2–3 layers of stacked thylakoids in the samples. Sometimes, clusters of plastoglobuli, indicating the previous presence of PLBs, were also observed as well as single stroma thylakoid layers running in parallel to each other. When compared with the same young chloroplasts exposed to 4-h-long dark salt treatment (instead of Hoagland treatment), we observed only very slight swelling of the intrathylakoidal space of the thylakoids (Figure 9B). However, the shape of the chloroplasts was rounded under salt stress (compare Figure 9A with 9B-D), indicating that the changes in the osmolarity and salt concentration in the medium indeed affected the plastids.

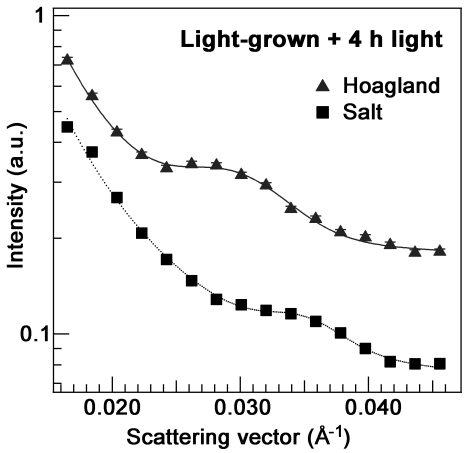

FIGURE 8 Typical radially averaged SANS curves of light-grown wheat leaf segments floated for 4 h in the light on Hoagland solution ('Hoagland') and 600 mM NaCl:KCl (1:1) solution ('Salt') (both dissolved in D_2O) and then measured in Hellma quartz cuvettes while being kept in the same solutions. Triangles and squares are measured data points (±SD); solid and dotted lines represent the fitted curves.

As the peculiar intensive swelling observed in the etioplasts of dark-grown wheat leaf segments treated for 4 h in the dark with salt (Figure 7B) was not observed in the young chloroplasts after 16 h of greening (Figure 9B), we decided to investigate at which stage of the

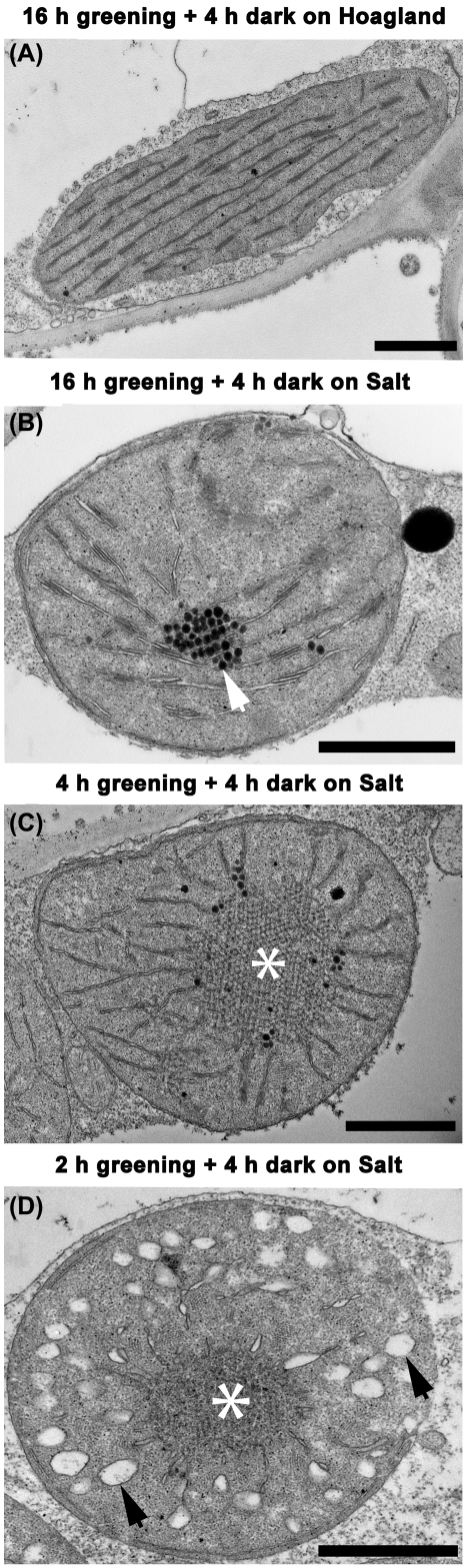

FIGURE 9 Transmission electron micrographs of typical plastid sections of intact dark-grown wheat seedlings first greened for 16 h (A, B), 4 h (C) or 2 h (D) on continuous light and then having their leaf segments floated for 4 h in the dark on Hoagland solution ('Hoagland') (A) or 600 mM NaCl:KCl (1:1) solution ("Salt") (B, C, D). Asterisk: prolamellar body; black arrowhead: swollen vesicles; white arrowhead: cluster of plastoglobuli. Scale bar: 1 μm.

etioplast-to-chloroplast transformation the stability of the plastid inner membranes increased. Therefore, we tested young chloroplasts of intact dark-grown wheat leaves greened for 4 h and 2 h, and then treated with the same salt stress for 4 h in the dark.

We observed no swelling after 4 h greening (Figure 9C). PLBs were present but no obvious PT swelling was observed after 4 h greening (Figure 9C). On the other hand, if the dark-grown leaves were greened only for 2 h, we observed swollen intrathylakoidal space in the (pro)thylakoids and slight irregularity in the PLB membranes (Figure 9D). Many swollen vesicles were present within the plastid stroma, especially at the periphery of the plastids.

3.6 | Monitoring lipid peroxidation by malondialdehyde measurements

The peculiar swelling of the thylakoid lumen is often linked to oxidative stress (Yamane et al., 2009). Therefore, we analyzed the lipid peroxidation of the studied samples. MDA is generated by the peroxidation of polyunsaturated fatty acids in plants. The MDA content of wheat leaf segments was significantly increased by salt treatment compared to the samples treated with Hoagland, except for the light-grown wheat leaf segments treated with salt for 4 h in the dark (Figure 10B, Table S2), which indicates that salt treatment induces oxidative stress in leaves having well-developed photosynthetic apparatus only in the light, but in the case of less developed chloroplasts or etioplasts also in the dark. PEG treatment for 4 h did not induce significant lipid peroxidation in any of the samples when compared with the samples floating on Hoagland.

3.7 | Monitoring lipid peroxidation by high-temperature thermoluminescence measurements

Thermoluminescence (TL) emission curves can be used to study photosynthetic electron transport (Vass & Govindjee, 1996) to monitor the effects of different biotic or abiotic stressors (Misra et al., 2012) and to examine lipid peroxidation (Ducruet & Vass, 2009). High-temperature thermoluminescence (HTTL) measurements provide a valuable tool to investigate the oxidative stress *in vivo* and its effect on the photosynthetic capacity by measuring low-level chemiluminescence emission. HTTL is in the same spectral range as chlorophyll fluorescence and PSII luminescence, but it is independent of pre-illumination; its signals usually appear in the 50 to 160°C region with usual peak maxima at 60–90°C and/or 105–140°C (Ducruet & Vass, 2009; Havaux & Niyogi, 1999).

We observed HTTL peaks in the dark-grown wheat leaf samples floating for 4 h in the dark (Figure 11A). TL bands appeared in the temperature region 80–115°C, 55–100°C and 75–105°C in Hoagland, salt and PEG solution, respectively. After 16 h greening of dark-grown leaves and subsequent 4-h-long dark treatment, we observed the appearance of a TL peak at 105°C in Hoagland, TL glow curve bands around 50 and 90°C in salt solution, while TL peaks were located around 60 and 100°C in PEG solution (Figure 11B). In the light-grown

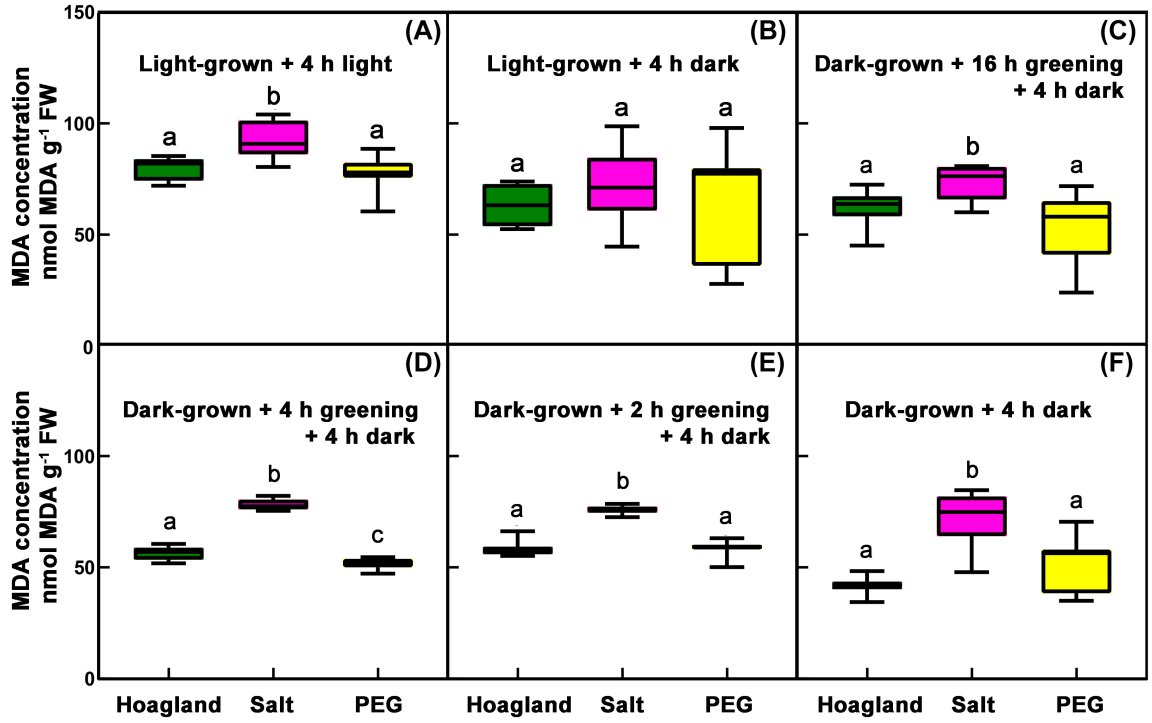

FIGURE 10 Malondialdehyde (MDA) concentrations on fresh mass (FW) basis of wheat leaf segments floated for 4 h in the light (A) or in the dark (B-F) on Hoagland solution ('Hoagland'), 600 mM NaCl:KCl (1:1) solution ('Salt') or isosmotic polyethylene glycol (PEG-6000, 'PEG') solution. (A,B) Leaf segments of light-grown seedlings; (C-F) leaf segments of intact dark-grown seedlings greened for 16 h (C), 4 h (D), 2 h (E) and 0 h (F) on continuous light and then treated for 4 h in the dark on the given solution. For each treatment, measurements were performed in 3–4 technical replicates in at least 3 different experiments (n = 9–12). Different letters indicate statistically significant differences between the samples according to Kruskal-Wallis nonparametric ANOVA followed by Dunn's multiple comparisons post hoc test or according to one-way-ANOVA followed by Tukey–Kramer multiple comparisons post hoc test in case data followed normal distribution ($P < 0.05$).

wheat leaf segments treated for 4 h in salt, PEG and Hoagland solution in the light, two distinct peaks (around 50–60°C and 90°C) appeared in salt and PEG treatment, and a shifted HTTL peak was detected around 105°C in Hoagland treatment (Figure 11C).

4 | DISCUSSION

Soil salinity is a continuously increasing global problem for agricultural crop production (Seleiman et al., 2019). Wheat is the second most important food crop, contributing to 55% of the carbohydrates and 20% of the calories consumed by mankind (Chattha et al., 2017). Therefore, understanding how salt stress affects the development and metabolism of wheat plants is of crucial importance. However, most literature data only deal with the effect of salt stress on fully developed plants, their photosynthetic performance and yield, seed germination, or seedling development in the light. Nevertheless, depending on the soil type, the used wheat cultivar, and the current agricultural protocols, wheat is sown at 5–10 cm depth in the soil, which means that the coleoptile-covered and later uncovered first leaves of developing etiolated seedlings are directly exposed to soil salinity. Seedlings in the soil are fully etiolated and only start greening when they reach the soil surface (Kakuszi et al., 2016; Vitányi et al., 2013) and are gradually exposed to light (Reinbothe et al., 2004). This way, salt stress may directly affect the structure and function of etioplasts, the etioplast-to-chloroplast transformation, all the intermediary plastid types and the seedling greening.

In previous studies, floating of the leaf segments of dark-grown seedlings of an Egyptian salt-sensitive wheat cultivar (*T. aestivum* cv. Giza 168) on 600 mM KCl:NaCl (1:1) solution in the dark for 4,5 h resulted in swelling of the PT lumen and strong inhibition of greening, Chl accumulation and etioplast-to-chloroplast transformation (Abdelkader et al., 2007a, 2007b, 2010). Salt stress induced either swelling (e.g., Yamane et al., 2004, 2008; Ounoki et al. 2021) or no swelling (e.g., Hasan et al., 2006; Hernández et al., 1995) of the intrathylakoidal space in the chloroplast. NaCl stabilized granum structure (Hasan et al., 2006; Ünnep et al., 2014), while KCl and KNO_3 treatment of isolated thylakoids resulted in shrinkage of the grana as revealed by SANS (Herdean et al., 2016). The swelling of the thylakoid lumen in chloroplasts was strongly associated with light-induced formation of reactive oxygen species and subsequent oxidative stress (Yamane et al., 2004, 2008; Hasan et al., 2005; Suo et al., 2017), while chloroplasts treated with salt in the dark showed no swelling (Mitsuya et al., 2000, 2003a). To clarify the reasons for the swelling of the inner membrane of plastids, we investigated how salinity, and its osmotic component, affected the inner membrane

system and activity of various plastid types: etioplasts, different stages of etioplast-to-chloroplast transformation and fully developed chloroplasts.

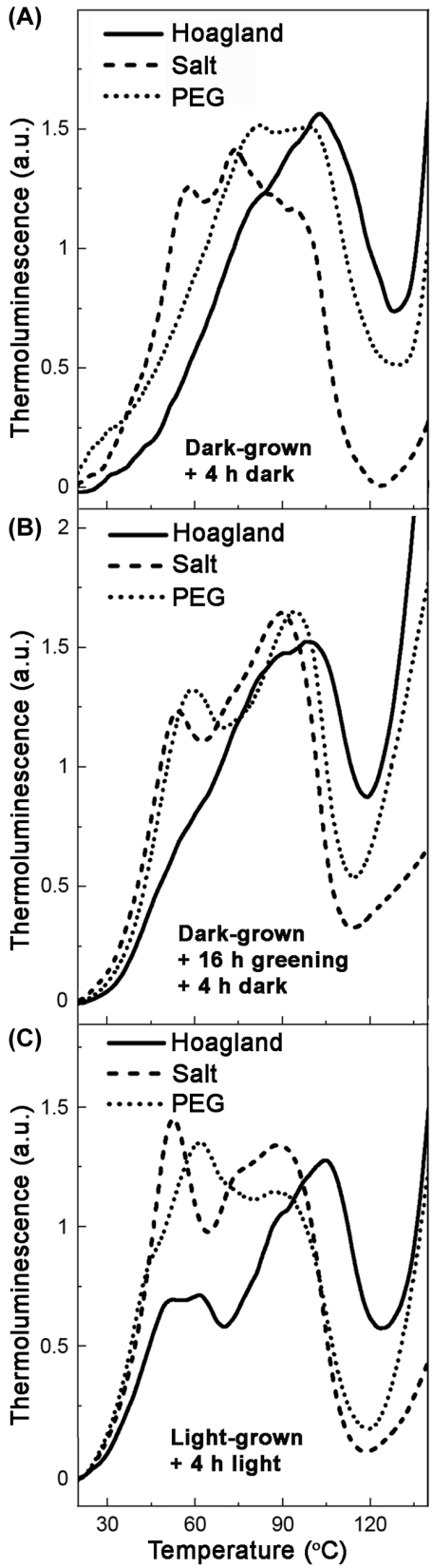

When compared with salt stress treatments, isosmotic PEG solutions only mildly, but often significantly, affected the measured physiological and biochemical parameters of chloroplasts and etioplasts (Tables S2-S3, Figures 2-6, 10, 11) but did not induce ultrastructural alterations in them (Table 1, Figure 7). The unchanged thylakoid structure under osmotic stress of wheat proteome agrees with the results of Chen et al. (2017). Though the increase in PSI-LHCII, the state transition specific complex (Pesaresi et al., 2009), may be artefactual because LHCII association is very sensitive to n-dodecyl-β-D-maltoside (Järvi et al., 2011; Sárvári et al., 2022), the higher amount of this complex (Figure 4) is in agreement with the results showing enhanced cyclic electron transport under osmotic or drought stress (Dulai et al., 2014; Lehtimäki et al., 2010). Taken together, our data indicate that the observed changes – first of all, the swelling of the PT lumen of etioplasts – are not associated with the osmotic stress induced by the high ion concentration of the applied solutions but must be connected with the direct and specific effects of the ions. Earlier investigations similarly confirmed the role of the ionic component in salinity-induced alterations of plastid structure and function in chloroplasts (Yamane et al., 2003; Miyake et al., 2006). However, to our knowledge, this is the first time that the same phenomenon has been studied and confirmed in etioplasts.

The applied short-term high-concentration salt treatment of the dark-grown leaf segments of the wheat cultivar Mv Béres gave similar results (Figure 7) to those of Abdelkader et al. (2007a) for the Giza 168 salt-sensitive wheat cultivar. The leaf segments lost their turgor and became highly fragile and prone to injuries during manipulation. This was in line with the observed plasmolysis of the cells, swelling of the PT lumen, and appearance of envelope invaginations in the etioplasts as described in Abdelkader et al. (2007a). Etioplasts also contained spotted bodies (Figure 7B), described as microtubule-like structures (Artus et al., 1990). 77 K fluorescence emission spectra indicated similar trends: the Hoagland and PEG-treated leaves had similar values, while the relative contribution of the emission of $Pchlide_{633}$ slightly increased under salt stress (Figure 3). It may be explained by HTTL data (Figure 11). The significantly increased MDA content (Figure 10) indicated lipid peroxidation in these etiolated samples (Figures 10,11).

Under our experimental conditions, light-grown wheat leaf segments treated with salt solution for 4 h in the dark did not show any visible changes in plastid ultrastructure (Figure 7), which is similar to

FIGURE 11 Thermoluminescence emission (normalized to the integrated area between 30 and 120°C) of wheat leaf segments floated for 4 h in the dark (A and B) or in the light (C) on Hoagland solution ('Hoagland'), 600 mM NaCl:KCl (1:1) solution ('Salt') or isosmotic polyethylene glycol (PEG-6000, 'PEG') solution. (A) Leaf segments of dark-grown seedlings; (B) leaf segments of intact dark-grown seedlings greened for 16 h on continuous light; (C) leaf segments of light-grown seedlings. 3–4 leaf segments were measured in the sample holder at once, 3 different measurements were performed per experiment and treatment. Experiments were repeated independently three times. Data show averaged curves of 3 independent experiments.

other data in the literature (Mitsuya et al., 2000, 2003a, 2003b). This is in line with the non-significant changes in the MDA contents (Figure 10), and the 77 K fluorescence emission spectra of the leaves (Figure 3). However, SPAD values (Table S1) and the organization of PSII slightly changed (Figure 4): PSII activity (Figures 2, 5 and 6) was lowered by salt stress, indicating a slight disturbance of this photosystem.

When the same light-grown wheat leaf segments were treated for 4 h in the light, the salt-induced alterations in the physiological and biochemical parameters were more pronounced (more strongly reduced Qy light and dark values, SPAD values, increased MDA content). These changes, along with the HTTL measurements (Figure 11), showed that oxidative stress and lipid peroxidation occurred in these samples. PSII organization was also somewhat more disturbed than in the dark treatment, as indicated by the disassembly of some megacomplexes and PSII-s and the decreased relative 77 K fluorescence emission at 685 and 695 nm (Figures 3 and 4). These data also confirm that PSII has higher sensitivity under stress conditions than PSI (Hameed et al., 2021; Dhokne *et al*., 2022).

At the same time, our TEM observations showed essentially unchanged chloroplast ultrastructure under salt stress applied for 4 h both in the dark or in the light (Figure 7). Fast Fourier Transformation (FFT) analysis of chosen granum areas of the micrographs (Table 1) and SANS measurements (Figure 8) have shown a decrease of the granum RD values, indicating shrinkage rather than dilatation or swelling under salt stress conditions, in line with some previous observations (Ünnep et al., 2014) and in contrast with other reports (Yamane et al., 2004, 2008; Hasan et al., 2005; Suo et al., 2017). The discrepancy of our data with the literature data might be explained by differences in the parameters of the salt stress treatment (our high concentration treatments being applied for a relatively short period of time, through floating of leaf segments) or the different salt sensitivity of the studied species.

Although these results have clarified that light can clearly aggravate the effects of the ionic component of salt stress in wheat leaves, further experiments were performed to answer why the inner membranes of etioplasts are more sensitive to salt stress treatment in the dark than chloroplasts, and at which stage of greening the etio-chloroplast inner membranes become less prone to the salt-stress induced swelling. When dark-grown plants were greened for 2 h only, we observed etio-chloroplasts with structures like etioplasts but with small peripheral vesicles and swollen (pro)thylakoid lumen (Figure 9D). After phototransformation and the subsequent Shibata shift, the slight red shift of the 77 K Chl fluorescence emission maximum started in Hoagland and PEG-treated leaves, while it did not occur in the salt-stressed samples (Figure 3). At this stage, the photosynthetic activity could not be detected even in the Hoagland-treated leaf segments (data not shown). In contrast, in plants greened for 4 h or 16 h and then treated for 4 h in the dark, the peculiar swelling of the intrathylakoidal space was no longer observed (Figures 9B-C). In these samples, the photosynthetic activity (Figures 5 and 6) and the main thylakoid complexes (Figure 3) appeared in young etio-chloroplasts or young chloroplasts as also described in the literature (Kanervo et al., 2008; Müller & Eichacker, 1999; Shevela et al., 2016). Nevertheless, salt stress strongly affected the greening of these plastids: the development of the Chl-protein complexes was slowed down as shown by the somewhat decreased PSII amount in thylakoids of 16-h-greened leaves and the lower PSI band in the 77 K fluorescence emission spectra, also containing a shoulder at 720 nm, referring potentially to the presence of PSI-core complexes (Lamb et al., 2018), compared to the Hoagland and PEG-treated samples in thylakoids of leaves greened for shorter times (Figure 3). The photosynthetic activity (Figures 5 and 6) decreased, while MDA (Figure 10) and HTTL measurements (Figure 11) indicated oxidative stress. However, at this stage or later stages of the greening, the plastids were already able to prevent the swelling of the intrathylakoidal space under salt treatment, even though PLBs were still present and re-formed during the 4 h dark treatment. As the disappearance of the swelling coincided with the appearance of the functionally active components of the photosynthetic electron transport (Kanervo et al., 2008; Müller & Eichacker, 1999; Shevela et al., 2016), we believe that it is probably the photosynthetic proton motive force and photosynthesis itself that stabilizes the membranes. However, the lipid and fatty acid composition of etioplasts is slightly altered during greening, and is slightly different in chloroplasts than in etioplasts (Armarego-Marriott et al., 2019; Fujii et al., 2019). Further investigations would be needed to elucidate whether these minor changes could have an influence on the salinity response of the different plastids or not.

The volume of the chloroplasts and their osmotic and ion homeostasis (e.g., K^+, Na^+ and Cl^-) needs to be strictly controlled (Pottosin & Dobrovinskaya, 2015). However, data in Arabidopsis show that some of the best characterized K^+, Cl^- transport components of the thylakoid membranes are highly expressed already in cotyledons, i.e., at early stages of plant development (Kunz et al., 2014). However, the amount of Na^+/H^+ antiporter in the envelope membrane of the chloroplast was found to be the highest at mature stage (Müller et al., 2014). Other authors report that the swelling of the intrathylakoidal space is induced by the influx of Cl^- from the plastid stroma to the lumen, and shrinkage is caused by the efflux of lumenal K^+ or Na^+ to the stroma (Pottosin & Shabala, 2016). Some data suggest that additional thylakoid Cl^- transport mechanisms exist in the light (Herdean et al., 2016). It is also possible that ion transport components of the thylakoids or the chloroplast envelope membrane may be upregulated by light in parallel to the biogenesis of thylakoid membranes. We should also mention that the observed stronger effects of salinity in salt-stressed light-grown leaf segments in the light might be related to increased transpiration or other processes that may result in enhanced ion uptake of chloroplasts under illumination (Nobel, 1967) when compared with data obtained in the dark. Nevertheless, according to our observations, the photosynthetically produced energy may be used to power the salt removal from the chloroplast/lumen. However, this issue may need further investigations.

5 | CONCLUSIONS

Taken together, our data have clearly demonstrated that the observed swelling of the PT lumen of the etioplasts is associated

with the ionic component of the salt stress, while isosmotic treatment with PEG had only slight effects on plastid structure and function. Also, we have shown that plastid inner membranes get stabilized, and the peculiar swelling disappears after 4 h greening of etioplasts (and a subsequent 4-h-long dark period), i.e., in parallel with the development of the functional photosynthetic apparatus during etioplast-to-chloroplast transformation. These results underline the importance of breeding wheat cultivars with improved etioplast membrane stability and increased tolerance to salt stress.

AUTHOR CONTRIBUTIONS

Conceptualization: Katalin Solymosi. Funding and resources: Katalin Solymosi, Győző Garab and Renáta Ünnep. Methodology, data curation, analysis, visualization: Roumaissa Ounoki (SPAD, photosynthetic activity measurements, 77 K fluorescence spectroscopy, thermoluminescence, MDA measurements, thylakoid isolation and gel electrophoresis, RD calculations based on TEM), Adél Sóti (77 K fluorescence spectroscopy, MDA measurements), Gábor Sipka and Győző Garab (thermoluminescence), Éva Sárvári (thylakoid isolation and gel electrophoresis), Katalin Solymosi (77 K fluorescence spectroscopy, TEM analyses), Renáta Ünnep (SANS). Writing of the original manuscript draft: Katalin Solymosi and Roumaissa Ounoki. Edited, approved and complemented by all authors.

ACKNOWLEDGMENTS

The authors are grateful to Csilla Gergely and Györgyi Balogh (Eötvös Loránd University) for skillful technical assistance with TEM sample preparation and gel electrophoresis, respectively. We would like to thank Brigitta Müller, Fruzsina Pankaczi, Deepali Rana and Ádám Solti (Department of Plant Physiology and Molecular Plant Biology, Eötvös Loránd University) for help with the MDA measurements. Expert advice of Gusztáv Schay (Semmelweis University, Budapest) for biostatistical analyses is also warmly acknowledged. We are highly indebted to Ottó Zsiros (Biological Research Center, Szeged) for help with plant growth for thermoluminescence experiments. This work was supported by the National Research, Development and Innovation Office (Grant OTKA FK 124748 to AS, ÉS, GG, KS, RO, RÜ). GG acknowledges partial support from the Czech Science Foundation (GA ČR 23-07744S), and RÜ acknowledges partial support of Grant OTKA PD 138540 (National Research, Development and Innovation Office). KS is grateful for the Bolyai János Research Scholarship of the Hungarian Academy of Sciences and for the support of the New National Excellence Programme of the Ministry of Culture and Innovation from the source of the National Research, Development and Innovation Fund. The Stipendium Hungaricum PhD scholarship of RO was financed by Tempus Public Foundation (Hungary).

FUNDING INFORMATION

National Research, Development and Innovation Office (Grant Award numbers: OTKA FK 124748, PD 138540), Czech Science Foundation (GA ČR 23-07744S).

DATA AVAILABILITY STATEMENT

The data that support the findings of this study are available upon reasonable request from the corresponding author.

ORCID

Roumaissa Ounoki https://orcid.org/0000-0002-8264-5288
Adél Sóti https://orcid.org/0009-0001-8294-9927
Renáta Ünnep https://orcid.org/0000-0001-5916-1974
Gábor Sipka https://orcid.org/0000-0002-8553-4890
Éva Sárvári https://orcid.org/0000-0003-1416-1860
Győző Garab https://orcid.org/0000-0002-3869-9959
Katalin Solymosi https://orcid.org/0000-0001-5246-2547

REFERENCES

Abdelkader, A. F., Aronsson, H., Solymosi, K., Böddi, B., & Sundqvist, C. (2007a). High salt stress induces swollen prothylakoids in dark-grown wheat and alters both prolamellar body transformation and reformation after irradiation. *Journal of Experimental Botany*, 58(10), 2553–2564.

Abdelkader, A. F., Aronsson, H., & Sundqvist, C. (2007b). High salt stress in wheat leaves causes retardation of chlorophyll accumulation due to a limited rate of protochlorophyllide formation. *Physiologia Plantarum*, 130(1), 157–166.

Abdelkader, A. F., Aronsson, H., & Sundqvist, C. (2010). Prolonged salt stress alters the ratios of protochlorophyllide spectral forms in dark-grown wheat (Triticum aestivum) and influences chlorophyll a accumulation following irradiation. *Acta Physiologiae Plantarum*, 32(5), 971–978.

Almásy, L. (2021). New measurement control software on the Yellow Submarine SANS instrument at the Budapest Neutron Centre. *Journal of Surface Investigation: X-Ray, Synchrotron and Neutron Techniques*, 15(3), 527–531.

Armarego-Marriott, T., Kowalewska, Ł., Burgos, A., Fischer, A., Thiele, W., Erban, A., Strand, D., Kahlau, S., Hertle, A., Kopka, J., Walther, D., Reich, Z., Schöttler, M. A., & Bock, R. (2019). Highly resolved systems biology to dissect the etioplast-to-chloroplast transition in tobacco leaves. *Plant Physiology*, 180(1), 654–681.

Artus, N. N., Ryberg, M., & Sundqvist, C. (1990). Plastid microtubule-like structures in wheat are insensitive to microtubule inhibitors. *Physiologia Plantarum*, 79(4), 641–648.

Basa, B., Lattanzio, G., Solti, Á., Tóth, B., Abadía, J., Fodor, F., & Sárvári, É. (2014). Changes induced by cadmium stress and iron deficiency in the composition and organization of thylakoid complexes in sugar beet (Beta vulgaris L.). *Environmental and Experimental Botany*, 101, 1–11.

Björkman, O., & Demmig, B. (1987). Photon yield of O2 evolution and chlorophyll fluorescence characteristics at 77 K among vascular plants of diverse origins. *Planta*, 170, 489–504.

Böddi, B., Ryberg, M., & Sundqvist, C. (1992). Identification of four universal protochlorophyllide forms in dark-grown leaves by analyses of the 77 K fluorescence emission spectra. *Journal of Photochemistry and Photobiology B: Biology*, 12(4), 389–401.

Candiano, G., Bruschi, M., Musante, L., Santucci, L., Ghiggeri, G. M., Carnemolla, B., Orecchia, P., Zardi, L., & Righetti, P. G. (2004). Blue silver: a very sensitive colloidal Coomassie G-250 staining for proteome analysis. *Electrophoresis*, 25(9), 1327–1333.

Chattha, M. U., Hassan, M. U., Khan, I., Chattha, M. B., Mahmood, A., Chattha, M. U., Nawaz, M., Subhani, M. N., Kharal, M., & Khan, S. (2017). Biofortification of wheat cultivars to combat zinc deficiency. *Frontiers in Plant Science*, 8, 1–8.

Chen, Y. E., Cui, J. M., Su, Y. Q., Zhang, C. M., Ma, J., Zhang, Z. W., Yuan, M., Liu, W. J., Zhang, H. Y., & Yuan, S. (2017). Comparison of phosphorylation and assembly of photosystem complexes and redox homeostasis in two wheat cultivars with different drought resistance. *Scientific Reports*, 7(1), 1–16.

Dhokne, K., Pandey, J., Yadav, R. M., Ramachandran, P., Rath, J. R., & Subramanyam, R. (2022). Change in the photochemical and structural organization of thylakoids from pea (Pisum Sativum) under salt stress. *Plant Physiology and Biochemistry*, 177, 46–60.

Ducruet, J. M., & Vass, I. (2009). Thermoluminescence: experimental. *Photosynthesis Research*, 101(2–3), 195–204.

Ducruet, J. M., & Vavilin, D. (1999). Chlorophyll high-temperature thermoluminescence emission as an indicator of oxidative stress: perturbating effects of oxygen and leaf water content. *Free Radical Research*, 31(1), 187–192.

Dulai, S., Molnár, I., Szopkó, D., Darkó, É., Vojtkó, A., Sass-Gyarmati, A., & Molnár-Láng, M. (2014). Wheat-Aegilops biuncialis amphiploids have efficient photosynthesis and biomass production during osmotic stress. *Journal of Plant Physiology*, 171(7), 509–517.

Franck, F., Eullaffroy, P., & Popovic, R. (1997). Formation of long-wavelength chlorophyllide (Chlide695) is required for the assembly of Photosystem II in etiolated barley leaves. *Photosynthesis Research*, 51(2), 107–118.

Fujii, S., Nagata, N., Masuda, T., Wada, H., & Kobayashi, K. (2019). Galactolipids are essential for internal membrane transformation during etioplast-to-chloroplast differentiation. *Plant & Cell Physiology*, 60(6), 1224–1238.

Füzi, J., Len, A., & Bajnok, K. (2017). *Research instruments at the Budapest Neutron Centre: Handbook of the central european training school on neutron techniques*. KFKI.

Goussi, R., Manaa, A., Derbali, W., Cantamessa, S., Abdelly, C., & Barbato, R. (2018). Comparative analysis of salt stress, duration and intensity, on the chloroplast ultrastructure and photosynthetic apparatus in Thellungiella salsuginea. *Journal of Photochemistry and Photobiology B: Biology*, 183, 275–287.

Grieco, M., Suorsa, M., Jajoo, A., Tikkanen, M., & Aro, E.-M. (2015). Light-harvesting II antenna trimers connect energetically the entire photosynthetic machinery — including both photosystems II and I. *Biochimica et Biophysica Acta (BBA) - Bioenergetics*, 1847(6), 607–619.

Hameed, A., Ahmed, M. Z., Hussain, T., Aziz, I., Ahmad, N., Gul, B., & Nielsen, B. L. (2021). Effects of salinity stress on chloroplast structure and function. *Cells*, 10(8).

Hasan, R., Kawasaki, M., Taniguchi, M., & Miyake, H. (2006). Salinity stress induces granal development in bundle sheath chloroplasts of maize, an NADP-malic enzyme-type C4 plant. *Plant Production Science*, 9(3), 256–265.

Hasan, R., Ohnuki, Y., Kawasaki, M., Taniguchi, M., & Miyake, H. (2005). Differential sensitivity of chloroplasts in mesophyll and bundle sheath cells in maize, an NADP-malic enzyme-type C4 plant, to salinity stress. *Plant Production Science*, 8(5), 567–577.

Havaux, M., & Niyogi, K. K. (1999). The violaxanthin cycle protects plants from photooxidative damage by more than one mechanism. *Proceedings of the National Academy of Sciences*, 96(15), 8762–8767.

Herdean, A., Teardo, E., Nilsson, A. K., Pfeil, B. E., Johansson, O. N., Ünnep, R., Nagy, G., Zsiros, O., Dana, S., Solymosi, K., Garab, G., Szabó, I., Spetea, C., & Lundin, B. (2016). A voltage-dependent chloride channel fine-tunes photosynthesis in plants. *Nature Communications*, 7, 11654.

Hernández, J. A., Olmos, E., Corpas, F. J., Sevilla, F., & del Río, L. A. (1995). Salt-induced oxidative stress in chloroplasts of pea plants. *Plant Science*, 105(2), 151–167.

Hoagland, D. R., & Arnon, D. I. (1950). The water-culture method for growing plants without soil. In *Circular of California Agricultural Experiment Station* (Vol. 347). University of California, College of Agriculture, Agricultural Experiment Station.

Järvi, S., Suorsa, M., Paakkarinen, V., & Aro, E. M. (2011). Optimized native gel systems for separation of thylakoid protein complexes: Novel super- and mega-complexes. *Biochemical Journal*, 439(2), 207–214.

Kakuszi, A., Sárvári, É., Solti, Á., Czégény, G., Hideg, É., Hunyadi-Gulyás, É., Bóka, K., & Böddi, B. (2016). Light piping driven photosynthesis in the soil: Low-light adapted active photosynthetic apparatus in the undersoil hypocotyl segments of bean (Phaseolus vulgaris). *Journal of Photochemistry and Photobiology B: Biology*, 161, 422–429.

Kalaji, H. M., Schansker, G., Brestic, M., Bussotti, F., Calatayud, A., Ferroni, L., Goltsev, V., Guidi, L., Jajoo, A., Li, P., Losciale, P., Mishra, V. K., Misra, A. N., Nebauer, S. G., Pancaldi, S., Penella, C., Pollastrini, M., Suresh, K., Tambussi, E., Bąba, W. (2017). Frequently asked questions about chlorophyll fluorescence, the sequel. *Photosynthesis Research*, 132(1), 13–66.

Kanervo, E., Singh, M., Suorsa, M., Paakkarinen, V., Aro, E., Battchikova, N., & Aro, E. M. (2008). Expression of protein complexes and individual proteins upon transition of etioplasts to chloroplasts in pea (Pisum Sativum). *Plant and Cell Physiology*, 49(3), 396–410.

Keiderling, U. (2002). The new 'BerSANS-PC' software for reduction and treatment of small angle neutron scattering data. *Applied Physics A*, 74(1), 1455–1457.

Kowalewska, Ł., Bykowski, M., & Mostowska, A. (2019). Spatial organization of thylakoid network in higher plants. *Botany Letters*, 166(3), 326–343.

Kunz, H. H., Gierth, M., Herdean, A., Satoh-Cruz, M., Kramer, D. M., Spetea, C., & Schroeder, J. I. (2014). Plastidial transporters KEA1, −2, and −3 are essential for chloroplast osmoregulation, integrity, and pH regulation in Arabidopsis. *Proceedings of the National Academy of Sciences of the United States of America*, 111(20), 7480–7485.

Lamb, J. J., Røkke, G., & Hohmann-Marriott, M. F. (2018). Chlorophyll fluorescence emission spectroscopy of oxygenic organisms at 77 K. *Photosynthetica*, 56(1), 105–124.

Lehtimäki, N., Lintala, M., Allahverdiyeva, Y., Aro, E.-M., & Mulo, P. (2010). Drought stress-induced upregulation of components involved in ferredoxin-dependent cyclic electron transfer. *Journal of Plant Physiology*, 167(12), 1018–1022.

Misra, A. N., Misra, M., & Ranjeet, S. (2012). Thermoluminescence in chloroplast thylakoid. In A. N. Misra (Ed.), *Biophysics* (pp. 155–170). IntechOpen.

Mitsuya, S., Kawasaki, M., Taniguchi, M., & Miyake, H. (2003a). Light dependency of salinity-induced chloroplast degradation. *Plant Production Science*, 6(3), 219–223.

Mitsuya, S., Kawasaki, M., Taniguchi, M., & Miyake, H. (2003b). Relationship between salinity-induced damages and aging in rice leaf issues. *Plant Production Science*, 6(3), 213–218.

Mitsuya, S., Takeoka, Y., & Miyake, H. (2000). Effects of sodium chloride on foliar ultrastructure of sweet potato (Ipomoea batatas Lam.) plantlets grown under light and dark conditions in vitro. *Journal of Plant Physiology*, 157(6), 661–667.

Miyake, H., Mitsuya, S., & Rahman, M. D. S. (2006). Ultrastructural effects of salinity stress in higher plants. In *Abiotic Stress Tolerance in Plants* (pp. 215–226).

Müller, B., & Eichacker, L. A. (1999). Assembly of the D1 precursor in monomeric photosystem II reaction center precomplexes precedes chlorophyll a-triggered accumulation of reaction center II in barley etioplasts. *The Plant Cell*, 11(12), 2365–2377.

Müller, M., Kunz, H. H., Schroeder, J. I., Kemp, G., Young, H. S., & Ekkehard Neuhaus, H. (2014). Decreased capacity for sodium export out of Arabidopsis chloroplasts impairs salt tolerance, photosynthesis and plant performance. *Plant Journal*, 78(4), 646–658.

Nagy, G., & Garab, G. (2021). Neutron scattering in photosynthesis research: recent advances and perspectives for testing crop plants. *Photosynthesis Research*, 150(1), 41–49.

Nobel, P. S. (1967). Relation of swelling and photophosphorylation to light-induced ion uptake by chloroplasts in vitro. *Biochimica et Biophysica Acta (BBA) - Bioenergetics*, 131(1), 127–140.

Ounoki, R., Ágh, F., Hembrom, R., Ünnep, R., Szögi-Tatár, B., Böszörményi, A., & Solymosi, K. (2021). Salt stress affects plastid ultrastructure and photosynthetic activity but not the essential oil composition in spearmint (Mentha spicata L. var. crispa "Moroccan"). *Frontiers in Plant Science*, 12(739467), 1–18.

Parihar, P., Singh, S., Singh, R., Singh, V. P., & Prasad, S. M. (2015). Effect of salinity stress on plants and its tolerance strategies. *Environmental Science and Pollution Research International*, 22(6), 4056–4075.

Pesaresi, P., Hertle, A., Pribil, M., Kleine, T., Wagner, R., Strissel, H., Ihnatowicz, A., Bonardi, V., Scharfenberg, M., Schneider, A., Pfannschmidt, T., & Leister, D. (2009). Arabidopsis STN7 kinase provides a link between short- and long-term photosynthetic acclimation. *The Plant Cell*, 21(8), 2402–2423.

Podmaniczki, A., Nagy, V., Vidal-Meireles, A., Tóth, D., Patai, R., Kovács, L., & Tóth, S. Z. (2021). Ascorbate inactivates the oxygen-evolving complex in prolonged darkness. *Physiologia Plantarum*, 171(2), 232–245.

Porra, R. J., Thompson, W. A., & Kriedemann, P. E. (1989). Determination of accurate extinction coefficients and simultaneous equations for assaying chlorophylls a and b extracted with four different solvents: verification of the concentration of chlorophyll standards by atomic absorption spectroscopy. *Biochimica et Biophysica Acta (BBA) - Bioenergetics*, 975(3), 384–394.

Pottosin, I., & Dobrovinskaya, O. (2015). Ion channels in native chloroplast membranes: challenges and potential for direct patch-clamp studies. *Frontiers in Physiology*, 6, 396.

Pottosin, I., & Shabala, S. (2016). Transport across chloroplast membranes: optimizing photosynthesis for adverse environmental conditions. *Molecular Plant*, 9(3), 356–370.

Rahman, S., Matsumuro, T., Miyake, H., & Takeoka, Y. (2000). Salinity-induced ultrastructural alterations in leaf cells of rice (Oryza sativa L.). *Plant Production Science*, 3(4), 422–429.

Reinbothe, C., Pollmann, S., Desvignes, C., Weigele, M., Beck, E., & Reinbothe, S. (2004). LHPP, the light-harvesting NADPH:protochlorophyllide (Pchlide) oxidoreductase:Pchlide complex of etiolated plants, is developmentally expressed across the barley leaf gradient. *Plant Science*, 167(5), 1027–1041.

Ryberg, M., & Sundqvist, C. (1982). Characterization of prolamellar bodies and prothylakoids fractionated from wheat etioplasts. *Physiologia Plantarum*, 56(2), 125–132.

Sárvári, É., Gellén, G., Sági-Kazár, M., Schlosser, G., Solymosi, K., & Solti, Á. (2022). Qualitative and quantitative evaluation of thylakoid complexes separated by Blue Native PAGE. *Plant Methods*, 18(1), 23.

Sárvári, É., & Nyitrai, P. (1994). Separation of chlorophyll-protein complexes by deriphat polyacrylamide gradient gel electrophoresis. *Electrophoresis*, 15(1), 1068–1071.

Schneider, C. A., Rasband, W. S., & Eliceiri, K. W. (2012). NIH Image to ImageJ: 25 years of image analysis. *Nature Methods*, 9(7), 671–675.

Seleiman, M. F., Kheir, A. M. S., Al-Dhumri, S., Alghamdi, A. G., Omar, E.-S. H., Aboelsoud, H. M., Abdella, K. A., & Abou El Hassan, W. H. (2019). Exploring optimal tillage improved soil characteristics and productivity of wheat irrigated with different water qualities. *Agronomy*, 9(5), 1–11.

Shevela, D., Arnold, J., Reisinger, V., Berends, H. M., Kmiec, K., Koroidov, S., Bue, A. K., Messinger, J., & Eichacker, L. A. (2016). Biogenesis of water splitting by photosystem II during de-etiolation of barley (Hordeum vulgare L.). *Plant Cell and Environment*, 39(7), 1524–1536.

Shrivastava, P., & Kumar, R. (2015). Soil salinity: a serious environmental issue and plant growth promoting bacteria as one of the tools for its alleviation. *Saudi Journal of Biological Sciences*, 22(2), 123–131.

Sipka, G., Magyar, M., Mezzetti, A., Akhtar, P., Zhu, Q., Xiao, Y., Han, G., Santabarbara, S., Shen, J.-R., Lambrev, P. H., & Garab, G. (2021). Light-adapted charge-separated state of photosystem II: structural and functional dynamics of the closed reaction center. *The Plant Cell*, 33(4), 1286–1302.

Smeller, L., Solymosi, K., Fidy, J., & Böddi, B. (2003). Activation parameters of the blue shift (Shibata shift) subsequent to protochlorophyllide phototransformation. *Biochimica et Biophysica Acta*, 1651(1–2), 130–138.

Solymosi, K., & Aronsson, H. (2013). Etioplasts and their significance in chloroplast biogenesis. In B. Biswal, K. Krupinska, & U. C. Biswal (Eds.), *Plastid Development in Leaves during Growth and Senescence* (pp. 39–71). SpringerNetherlands.

Solymosi, K., & Schoefs, B. (2010). Etioplast and etio-chloroplast formation under natural conditions: The dark side of chlorophyll biosynthesis in angiosperms. *Photosynthesis Research*, 105(2), 143–166.

Suo, J., Zhao, Q., David, L., Chen, S., & Dai, S. (2017). Salinity response in chloroplasts: Insights from gene characterization. *International Journal of Molecular Sciences*, 18(5), 1–17.

Turan, S., & Tripathy, B. C. (2015). Salt-stress induced modulation of chlorophyll biosynthesis during de-etiolation of rice seedlings. *Physiologia Plantarum*, 153(3), 477–491.

Ünnep, R., Zsiros, O., Solymosi, K., Kovács, L., Lambrev, P. H., Tóth, T., Schweins, R., Posselt, D., Székely, N. K., Rosta, L., Nagy, G., & Garab, G. (2014). The ultrastructure and flexibility of thylakoid membranes in leaves and isolated chloroplasts as revealed by small-angle neutron scattering. *Biochimica et Biophysica Acta - Bioenergetics*, 1837(9), 1572–1580.

Vass, I., & Govindjee. (1996). Thermoluminescence from the photosynthetic apparatus. *Photosynthesis Research*, 48(1–2), 117–126.

Vitányi, B., Kósa, A., Solymosi, K., & Böddi, B. (2013). Etioplasts with protochlorophyll and protochlorophyllide forms in the under-soil epicotyl segments of pea (Pisum sativum) seedlings grown under natural light conditions. *Physiologia Plantarum*, 148(2), 307–315.

von Arnim, A., & Deng, X. W. (1996). A role for transcriptional repression during light control of plant development. *BioEssays*, 18(11), 905–910.

Yamane, K., Kawasaki, M., Taniguchi, M., & Miyake, H. (2003). Differential effect of NaCl and polyethylene glycol on the ultrastructure of chloroplasts in rice seedlings. *Journal of Plant Physiology*, 160(5), 573–575.

Yamane, K., Kawasaki, M., Taniguchi, M., & Miyake, H. (2008). Correlation between chloroplast ultrastructure and chlorophyll fluorescence characteristics in the leaves of rice (Oryza sativa L.) grown under salinity. *Plant Production Science*, 11(1), 139–145.

Yamane, K., Mitsuya, S., Kawasaki, M., Taniguchi, M., & Miyake, H. (2009). Antioxidant capacity and damages caused by salinity stress in apical and basal regions of rice leaf. *Plant Production Science*, 12(3), 319–326.

Yamane, K., Rahman, M. S., Kawasaki, M., Taniguchi, M., & Miyake, H. (2004). Pretreatment with antioxidants decreases the effects of salt stress on chloroplast ultrastructure in rice leaf segments (Oryza sativa L.). *Plant Production Science*, 7(3), 292–300.

Yokono, M., Takabayashi, A., Akimoto, S., & Tanaka, A. (2015). A megacomplex composed of both photosystem reaction centres in higher plants. *Nature Communications*, 6(1), 6675.

Yokono, M., Takabayashi, A., Kishimoto, J., Fujita, T., Iwai, M., Murakami, A., Akimoto, S., & Tanaka, A. (2019). The Psi–PSII megacomplex in green plants. *Plant and Cell Physiology*, 60(5), 1098–1108.

SUPPORTING INFORMATION

Additional supporting information can be found online in the Supporting Information section at the end of this article.

How to cite this article: Ounoki, R., Sóti, A., Ünnep, R., Sipka, G., Sárvári, É., Garab, G. et al. (2023) Etioplasts are more susceptible to salinity stress than chloroplasts and photosynthetically active etio-chloroplasts of wheat (*Triticum aestivum* L.). *Physiologia Plantarum*, 175(6), e14100. Available from: https://doi.org/10.1111/ppl.14100